Coupled solitons in resonant Raman interaction of intense polaritons

A. L. Ivanov and H. Haug
Institut für Theoretische Physik, J. W. Goethe Universität Frankfurt, Robert-Mayer-Strasse 8, D-60054 Frankfurt, Germany

G. S. Vygovskii
All-Russian Research Institute for Metrological Service, Gosstandar, Andreevskaya naberezhnayia 2, Moscow 117965, Russia
(Received 28 November 1995)

The generation of three-wave solitons (TWS's) in the resonant LO-phonon – mediated interaction of two intense coherent polaritons is proposed and analyzed. These TWS's consist of the mutually coupled two polariton and LO-phonon nonlinear waves and propagate without dispersive spreading with an anomalous soliton velocity. Starting with an initial microscopic picture of the exciton – LO-phonon Fröhlich interaction and exciton-photon polariton coupling in polar direct-band-gap semiconductors, we derive a closed set of five macroscopic equations for a resonant triplet: polariton 1 — polariton 2 — LO phonon. An adequate method of finding the fundamental TWS's of these nonlinear equations is developed. This approach treats the LO-phonon – mediated polariton-polariton interaction beyond the standard perturbation theory, which deals with the lowest nonlinear susceptibilities $\chi^{(2)}$ and $\chi^{(3)}$. A classification of the fundamental Raman solitons by their dispersion is given in terms of *quasipolariton* and *quasiphonon* TWS's. For the quasipolariton TWS's, one of the mutually coupled nonlinear polaritons is a giant parametric solitary pulse, the common soliton velocity v_s decreases with the intensities of the polaritons. The quasiphonon Raman TWS's have no analogy in classical nonlinear optics. These coupled solitons are accompanied by a giant LO-phonon solitary pulse, and v_s increases with the optical pump intensity. [S0163-1829(96)06419-3]

I. INTRODUCTION

For more than two decades, polariton solitons in bulk semiconductors have been an intriguing problem in solid state nonlinear optics. Single-mode polariton solitons due to self-interaction of an intense coherent polariton have been modeled in detail (see, e.g., Refs. 1). The optical nonlinearity responsible for these solitons originates from the effective Coulombic interaction between virtual excitons of the coherent polariton. These polariton solitons are at the same time a manifestation of the optical exciton Stark effect[2] in self-interaction of the pump polariton. The Keldysh set of two macroscopic equations,[3] the Maxwell equation and the equation for the polarization with a Kerr-type nonlinear term $\propto|P|^2P$ (P is the excitonic polarization), is well-suited for the corresponding theoretical analysis. However, up until now there has not been clear-cut experimental evidence for single-mode polariton solitons.

In the present work, we analyze the coupled traveling solitons in resonant LO-phonon mediated interaction between two coherent excitonic polaritons. Such coupled solitons are similar to *Raman solitons* recently observed in rotational and vibrational stimulated Raman scattering (SRS) in CO_2-pumped para-H_2.[4–6] A so-called anomalous pump-depletion reversal coupled to a corresponding dark soliton in the quasi-continous-wave background of the Stokes signal represents an observable structure of the Raman solitons. The theory of Raman solitons has been developed in detail[7,8] within a generalized set of the Maxwell-Bloch equations.

Two important features, the polariton effect and the translational invariance of a crystal lattice, distinguish three-wave interaction in semiconductors from mentioned above SRS in molecular optics. The incoming light, which resonates with an exciton level, induces a polariton consisting of the exciton and photon components.[9] Each of these components requires, in principle, a separate description in Raman scattering. Only the excitonic component, i.e., the polarization, couples with the phonon field. Due to translational invariance, bulk phonons are characterized by their wave vectors and dispersion. Therefore, the momentum conservation holds in Raman scattering of polaritons.

In resonant Raman interaction (RRI), the two coherent polaritons and resonant LO phonon are treated on an equal basis within the coupled macroscopic wave equations. Because each of the interacting fields has a well-defined carrier wave vector, we refer the coupled polariton Raman solitons to three-wave solitons (TWS's). A theory of electromagnetic TWS's has been developed already in the early days of nonlinear optics,[10] within coupled nonlinear wave equations for the electric light fields. This phenomenological model operates with the lowest-order nonlinear susceptibility $\chi^{(2)}$.

Two of the nonlinear waves of the polariton TWS's are solitary. These coupled solitary waves, or bright solitons, form a steady-state traveling nonlinear perturbation in a cw background of the third wave, which can be treated as a nonlinear pump wave. The most interesting case corresponds to a lower-frequency pump polariton in the resonant triplet. In this case, the solitary LO phonon is generated by an exchange of virtual excitons between the two intense polaritons in coherent phonon-mediated RRI. For the coupled polariton solitons, the leading half part of the solitary polariton initiates stimulated inverse Raman scattering, while its trailing half part is involved in stimulated normal scattering. This scenario of the energy exchange between nonlinear waves, which is similar to self-induced transparency in the system of two-level atoms, is characteristic for TWS's.[5]

The dispersion of the solitary polariton in the resonant triplet of TWS's reveals a rich and complicated structure. It originates from the mutual hybridization of the initial polariton and LO-phonon dispersions, similarly as the polariton dispersion develops from the exciton and photon spectra. This dynamical renormalization of the spectrum relates to the *phonoriton* transient excitations of a semiconductor in the presence of the given intense coherent polariton.[11–16] The phonoriton dispersion follows dynamically the optical pump intensity and gives rise to the phonon-mediated exciton optical Stark effect.[12] However, for the Raman TWS's the renormalized dispersion is even more complicated than that of the phonoriton, because the two coupled nonlinear polaritons have comparable intensities. The renormalized spectrum of the solitary polariton consists of several separate dispersion branches. Parts of them approach the unperturbed polariton branches, while the other branches are close to the initial LO-phonon dispersion shifted by the carrier frequency of the pump polariton. This property gives rise to the natural classification of polariton TWS's.

II-VI direct-band-gap polar semiconductors like CdS and CdSe possess a well-developed polariton effect, as well as a strong exciton–LO-phonon Fröhlich coupling. These ionic crystals are, therefore, well suited for the generation of the coupled polariton solitons in RRI. Due to the large optical nonlinearities and high optical densities in the semiconductors, the scales for the time, the optical length and the pump intensity reduce from ns, m, and GW/cm^2, respectively, for Raman solitons in molecular optics[4–6] to ps, μm, and MW/cm^2 for the polariton Raman TWS's. For moderate optical excitations, the phonon-mediated exciton-exciton coupling in RRI should be more pronounced than the exciton-exciton Coulombic interaction, due to its *resonant* character. Therefore, we expect the polariton TWS's, with its rather specific signatures, to be observed more easily than the single-mode polariton solitons. Moreover, an observation of related polariton solitons in a resonant exciton-biexciton three-wave interaction has been already reported.[17]

In Sec. II, we discuss the initial exciton-photon–LO-phonon microscopic Hamiltonian of ionic direct-band-gap semiconductors in the presence of a well-developed polariton effect and strong exciton–LO-phonon Fröhlich coupling. The closed set of five macroscopic equations for the exciton and photon components of two interacting coherent polaritons and the correspondong resonant LO phonon is derived on the basis of this Hamiltonian. Various limiting cases of these basic equations, i.e., Hopfield's polariton equations, the equations for spontaneous polariton Raman scattering, and the phonoriton macroscopic equations, are discussed.

In Sec. III, we costruct the simplest traveling nonlinear solutions of the five basic equations. The main point is to reduce the initial set to three coupled equations for the *polarization* fields, for which analytic solutions for the fundamental traveling TWS's are derived. Three relationships between seven initial parameters are established. We specify the four free parameters in accordance with possible experiments.

In Sec. IV, the relationships between the initial parameters of the TWS's are examined. We classify the fundamental coupled TWS's by the dispersion of the solitary polariton. The quasipolariton and quasiphonon TWS's with different physical properties are introduced.

In Sec. V, the quasipolariton fundamental TWS's are analyzed. In the coupled resonant triplet, the solitary polariton is a giant parametric pulse, while both the dark (dip) and antidark (spike) solitons can be formed in the cw background of the pump nonlinear polariton, depending on the scattering geometry.

In Sec. VI, we investigate the quasiphonon TWS's within a generalized set of the reduced polarization equations. In the quasiphonon TWS's, the exciton and photon components decouple from the polariton balance. In this case, the TWS's actually consist of four components. Now, one has to describe separately the exciton (polarization) and photon (electromagnetic field) components of the nonlinear pump polariton. The unusual properties of the quasiphonon TWS's are analyzed.

In Sec. VII, the stabilities of the quasiphonon and quasipolariton TWS's are examined. We discuss also possible experiments on polariton Raman TWS's. A brief discussion of an adoptation of our model to the polariton TWS's in nonpolar conjugated polymers and III-V compound semiconductors concludes this section.

II. MODEL

The initial microscopic Hamiltonian is given by

$$H=H_0+H_{x-\gamma}+H_{x-\mathrm{ph}},$$

$$H_0=\sum_{\mathbf{p}}\hbar[\omega^x(p)B_{\mathbf{p}}^{\dagger}B_{\mathbf{p}}+\omega^{\gamma}(p)\alpha_{\mathbf{p}}^{\dagger}\alpha_{\mathbf{p}}+\Omega_0 c_{\mathbf{p}}^{\dagger}c_{\mathbf{p}}],$$

$$H_{x-\gamma}=\sum_{\mathbf{p}}\left\{i\frac{\hbar\Omega_c}{2}\left[\frac{\omega_t}{\omega^{\gamma}(p)}\right]^{1/2}(\alpha_{\mathbf{p}}^{\dagger}+\alpha_{-\mathbf{p}})(B_{\mathbf{p}}-B_{-\mathbf{p}}^{\dagger})+\frac{\hbar\Omega_c^2}{4\omega^{\gamma}(p)}(\alpha_{\mathbf{p}}^{\dagger}+\alpha_{-\mathbf{p}})(\alpha_{\mathbf{p}}+\alpha_{-\mathbf{p}}^{\dagger})\right\},$$

$$H_{x-\mathrm{ph}}=\sum_{\mathbf{p},\mathbf{k}}i\hbar M_{x-\mathrm{ph}}(\mathbf{p}-\mathbf{k})[B_{\mathbf{p}}^{\dagger}B_{\mathbf{k}}(c_{\mathbf{p}-\mathbf{k}}-c_{-\mathbf{p}+\mathbf{k}}^{\dagger})], \quad (1)$$

where $B_{\mathbf{p}}$, $\alpha_{\mathbf{p}}$, and $c_{\mathbf{p}}$ are the exciton, photon, and optical phonon operators, respectively; $\omega^x(p)=\omega_t+p^2/2M$, $\omega^{\gamma}(p)=cp/\sqrt{\varepsilon_g}$, and Ω_0 are the corresponding dispersions; ε_g is the background optical dielectric constant for the exciton resonance; M is the exciton translational mass; $\hbar\omega_t$ is the energy of a transverse exciton. Two basic interactions, exciton-photon $H_{x\text{-}\gamma}$ and exciton-phonon $H_{x\text{-ph}}$, enter the Hamiltonian (1), which describe the exciton-photon-phonon system of a direct-band-gap semiconductor.

The Hamiltonian $H_{x\text{-}\gamma}$ of Eq. (1) describes the exciton-transverse light field interaction, which follows the momentum conservation. The oscillator strength Ω_c (polariton parameter) of the exciton-photon coupling is determined by

$$\Omega_c=2\sqrt{2\pi}\frac{e}{\sqrt{\hbar\omega_t}}\left(\frac{p_{cv}}{m_0}\right)\tilde{\phi}_0(\mathbf{r}=0)=\left(\frac{4\pi\tilde{\beta}}{\varepsilon_g}\right)^{1/2}\omega_t=\sqrt{2\omega_{lt}\omega_t}, \quad (2)$$

where $\widetilde{\beta}$ is the dimensionless polariton oscillator strength, ω_{lt} is the polariton longitudinal-transverse splitting, $\widetilde{\phi}_0(\mathbf{r})$ is the exciton ground state wave function in real space, $p_{cv}=-\langle u_{\mathbf{p},c}|\nabla|u_{-\mathbf{p},v}\rangle$ is the momentum matrix element between the Bloch functions of the conduction and valence bands. $H_0+H_{x-\gamma}$ reduces to Hopfield's quadratic Hamiltonian.[9] Formally, a polariton is an eigenstate of this quadratic form.

Raman spectroscopy of semiconductors is well developed.[18] Raman scattering of excitons is determined both by the deformation potential (DP) and by the Fröhlich ($\mathscr{F}$) mechanism.[18,19] The short-range DP mechanism gives rise to ''allowed'' Raman processes, which are independent of the scattering angle. The $\mathscr{F}$ mechanism stems from the macroscopic electric field, which accompanies a LO phonon in polar semiconductors, and determines ''forbidden'' Raman scattering with $M_{x\text{-ph}}(\mathbf{p}-\mathbf{k})\propto|\mathbf{p}-\mathbf{k}|$ in the Hamiltonian $H_{x\text{-ph}}$ (Ref. 20). $\mathscr{F}$ forbidden Raman scattering strongly dominates in a spectral vicinity of the exciton resonance in polar semiconductors.[21] Only this mechanism is included in our model as responsible for the resonant phonon-mediated interaction of the polaritons.

The matrix element $M_{x\text{-ph}}(\mathbf{p}-\mathbf{k})$ of the exciton–LO-phonon $\mathscr{F}$ interaction, which involves the ground exciton level $n=1$ in intraband $\mathscr{F}$ scattering, is given by[20]

$$M_{x\text{-ph}}(\mathbf{p}-\mathbf{k})=\mathscr{S}\left[\frac{\hbar}{2\Omega_0 V}\right]^{1/2}|\mathbf{p}-\mathbf{k}|,$$

$$\mathscr{S}=\Omega_0\left[\pi\left(\frac{m_e-m_h}{M}\right)^2\left(\frac{\varepsilon_0}{\varepsilon_\infty}-1\right)\frac{a_x^3}{\mu}\right]^{1/2}, \tag{3}$$

where V is the crystal volume, a_x is the exciton Bohr radius, ε_0 is the static dielectric constant, ε_∞ is the high-frequency dielectric constant for the LO-phonon resonance, $\mathbf{p}-\mathbf{k}$ is the phonon wave vector, m_e (m_h) is the electron (hole) mass ($M=m_e+m_h$), and μ is the reduced exciton mass. Equation (3) is valid for a small momentum transfer $|\mathbf{p}-\mathbf{k}|a_x\ll 1$. Here, $\mathbf{p}$ and $\mathbf{k}$ are the wave vectors of the polaritons with polarizations $\mathbf{e}_\mathbf{p}$ and $\mathbf{e}_\mathbf{k}$, respectively, which are involved in RRI. The intraband $\mathscr{F}$ mechanism contributes only to diagonal $\mathbf{e}_\mathbf{p}\|\mathbf{e}_\mathbf{k}$ RRI, irrespective of the crystal symmetry, if the excitons are assumed to be isotropic.[21]

In order to investigate the simplest TWS's, we restrict ourselves to the one-dimensional (1D) geometry with $\mathbf{p}\|\mathbf{k}$. The corresponding closed set of the macroscopic equations for the positive-frequency components of the electric fields $E_{j=1,2}(\xi,t)$ and excitonic polarizations $P_{j=1,2}(\xi,t)$ of the two interacting polaritons and for the scalar potential $\Phi(\xi,t)$ of the resonant LO phonon is given by

$$\left[\frac{\varepsilon_g}{c^2}\frac{\partial^2}{\partial t^2}-\frac{\partial^2}{\partial\xi^2}\right]E_1^{(+)}(\xi,t)=-\frac{4\pi}{c^2}\frac{\partial^2}{\partial t^2}P_1^{(+)}(\xi,t), \tag{4a}$$

$$\left[\frac{\partial^2}{\partial t^2}+\frac{1}{2}\Gamma^x\frac{\partial}{\partial t}+\omega_t^2-\frac{\hbar\omega_t}{2M}\frac{\partial^2}{\partial\xi^2}\right]P_1^{(+)}(\xi,t)$$

$$=\omega_t^2\widetilde{\beta}E_1^{(+)}(\xi,t)-\omega_t\sqrt{\rho}\mathscr{S}P_2^{(+)}(\xi,t)\frac{\partial^2}{\partial\xi^2}\Phi^{(+)}(\xi,t), \tag{4b}$$

$$\left[\frac{\partial^2}{\partial t^2}+\frac{1}{2}\Gamma^{\mathrm{ph}}\frac{\partial}{\partial t}+\Omega_0^2\right]\Phi^{(+)}(\xi,t)$$

$$=\frac{\mathscr{S}}{\sqrt{\rho}\omega_t\widetilde{\beta}}P_2^{(-)}(\xi,t)P_1^{(+)}(\xi,t), \tag{4c}$$

$$\left[\frac{\varepsilon_g}{c^2}\frac{\partial^2}{\partial t^2}-\frac{\partial^2}{\partial\xi^2}\right]E_2^{(+)}(\xi,t)=-\frac{4\pi}{c^2}\frac{\partial^2}{\partial t^2}P_2^{(+)}(\xi,t), \tag{4d}$$

$$\left[\frac{\partial^2}{\partial t^2}+\frac{1}{2}\Gamma^x\frac{\partial}{\partial t}+\omega_t^2-\frac{\hbar\omega_t}{2M}\frac{\partial^2}{\partial\xi^2}\right]P_2^{(+)}(\xi,t)$$

$$=\omega_t^2\widetilde{\beta}E_2^{(+)}(\xi,t)-\omega_t\sqrt{\rho}\mathscr{S}P_1^{(+)}(\xi,t)\frac{\partial^2}{\partial\xi^2}\Phi^{(-)}(\xi,t). \tag{4e}$$

Here, ξ is the coordinate axis along the direction of propagation, $\Gamma^x/2$ and $\Gamma^{\mathrm{ph}}/2$ are the inverse coherence lifetimes of excitons and LO phonons, respectively, and the macroscopic fields are defined by

$$\mathbf{E}(\mathbf{r},t)=\mathbf{E}^{(+)}(\mathbf{r},t)+\mathbf{E}^{(-)}(\mathbf{r},t)$$

$$=\sum_\mathbf{p}\left(\frac{2\pi\hbar cp}{V}\right)^{1/2}i\mathbf{e}_\mathbf{p}[\alpha_\mathbf{p}(t)e^{i\mathbf{pr}}-\alpha_\mathbf{p}^\dagger(t)e^{-i\mathbf{pr}}],$$

$$\mathbf{P}(\mathbf{r},t)=\mathbf{P}^{(+)}(\mathbf{r},t)+\mathbf{P}^{(-)}(\mathbf{r},t)=\sum_\mathbf{p}\left(\frac{\hbar\omega_t\widetilde{\beta}}{2V}\right)^{1/2}\mathbf{e}_\mathbf{p}[B_\mathbf{p}(t)e^{i\mathbf{pr}}$$

$$+B_\mathbf{p}^\dagger(t)e^{-i\mathbf{pr}}],$$

$$\Phi(\mathbf{r},t)=\Phi^{(+)}(\mathbf{r},t)+\Phi^{(-)}(\mathbf{r},t)=\sum_\mathbf{p}\left(\frac{\hbar}{2\rho V\Omega_0 p^2}\right)^{1/2}(-i)$$

$$\times[c_\mathbf{p}(t)e^{i\mathbf{pr}}-c_\mathbf{p}^\dagger(t)e^{-i\mathbf{pr}}], \tag{5}$$

where ρ is the crystal density. The LO-phonon scalar potential $\Phi^{(+)}(\xi,t)$ determines the corresponding lattice displacement field $u^{(+)}(\xi,t)$ by $u^{(+)}(\xi,t)=\partial\Phi^{(+)}(\xi,t)/\partial\xi$. Equations (4a)–(4e) for the coherent macroscopic fields are derived from the initial Hamiltonian (1) within a method developed in Refs. 11 and 15.

Equations (4a) and (4b) describe the *first* polariton (E_1 and P_1) in the resonant triplet. The wave equation (4a) for the electric component E_1 contains the linear source on the right-hand side (r.h.s.), due to the excitonic polarization P_1. The first term on the r.h.s. of the polarization Eq. (4b) couples the excitons with the resonant light, while the second one stems from the RRI of the two coherent polaritons. Equations (4d) and (4e), which describe the *second* polariton (E_2 and P_2) in the RRI, have the similar physical interpretation. Finally, Eq. (4c) describes the evolution of the coherent LO phonon, which is generated in the RRI of the two polaritons. The macroscopic Eqs. (4a)–(4e) are derived under the assumption that the carrier frequency ω of the polariton 1 belongs to a spectral vicinity of the anti-Stokes resonance $\omega_\mathbf{k}+\Omega_0$ of the polariton 2 with the carrier frequency $\omega_\mathbf{k}$, i.e., $\omega\simeq\omega_\mathbf{k}+\Omega_0$.

Equations (4a) and (4b) and (4c)–(4e) reduce to the two independent identical sets of Hopfield's polariton equations,[9] if one neglects the $\mathscr{F}$ exciton–LO-phonon interaction, i.e., sets $\mathscr{S}=0$. Then, the linear macroscopic Eqs.

(4a) and (4b) [or Eqs. (4c)–(4e)] with $\mathscr{L}=0$ describe the first (second) free polariton. In order to treat spontaneous Raman scattering (SRS) of polariton 1, one can use Eqs. (4c)–(4e). In this case, the first polariton $(E_1(\xi,t), P_1(\xi,t))$ has to be considered as a given pulse, while the Stokes polariton 2 (E_2,P_2) is a small signal. The main feature of this approach to SRS is an explicit inclusion of the polariton effects. The corresponding theory of SRS is developed, e.g., in Ref. 22. If the coherent polariton 2 is considerably stronger than the first one, Eqs. (4a)–(4e) decouple into the two independent sets of Eqs. (4a)–(4c) and Eqs. (4d) and (4e). Then, the second polariton is a given coherent pump wave with the polarization $P_2=P_{02}\exp(-i\omega_{\mathbf{k}}t+ik\xi)$ and Eqs. (4a)–(4c) describe the phonoriton excitations[11–16] of a semiconductor. The phonoriton dispersion, i.e., the dynamical coherent photon–exciton–LO-phonon spectrum, develops in the spectral vicinity of the anti-Stokes resonance $\omega_{\mathbf{k}}+\Omega_0$ of the pump polariton 2.

The approximation of the single intermediate exciton state $n=1$ for RRI holds if $\Omega_0 \ll \Omega_c$. With increasing exciton radius (decreasing exciton binding energy ϵ^x), this approximation becomes invalid, because the polariton parameter $\Omega_c \propto a_x^{-3/2}$ [see Eq. (2)] decreases. On the other hand, according to Eq. (3) the matrix element $M_{x-\mathrm{ph}} \propto a_x^{-3/2}$, i.e., an increase of a_x results in an enhancement of the $\mathscr{T}$ interaction. It seems that CdS and CdSe direct-band-gap polar semiconductors are best suited for the compromise between these opposite trends. For CdS, e.g., $\hbar\Omega_c \simeq 140$ meV and $\hbar\Omega_0 \simeq 38$ meV, while $|\mathbf{p}-\mathbf{k}|a_x \simeq 0.1$ – 0.2. Therefore, the macroscopic Eqs. (4a)–(4e) are appropriate for the description of plane-wave RRI in CdS and CdSe in the geometry $\mathbf{e_p} \| \mathbf{e_k}$ and $\mathbf{p} \| \mathbf{k} \| \boldsymbol{\xi} \perp \mathbf{c}$ axis of a crystal.

Mathematically, the five Eqs. (4a)–(4e) are the nonlinear set of a generalized type for Raman solitons. Conventional studies of the TWS's (Ref. 10) deal with three nonlinear wave equations for the light fields resonantly coupled, due to the lowest-order nonlinear susceptibility $\chi^{(2)}$. In the macroscopic Eqs. (4a)–(4e) the nonlinear terms are presented only in the ''matter'' Eqs. (4b), (4c), and (4e). The main point of our approach is that one cannot analyze RRI by means of perturbation theory for high intensities I_1 and I_2 of the coherent polaritons.[11,15] Equations (4a)–(4e) include explicitly the entire series of the nonlinear susceptibilities $\chi^{(n)}$, within the initial microscopic model given by the Hamiltonian (1).

III. NONLINEAR TRAVELING SOLUTIONS OF THE MACROSCOPIC EQUATIONS

For further analysis, we will concentrate on the simplest traveling TWS's solutions of the set of Eqs. (4a)–(4e). These nonlinear solutions are also called the *fundamental* solitons. The fundamental Raman TWS's describe three coupled elementary nonlinear waves, two polaritons and one LO phonon, propagating without dispersive spreading with a common group velocity v_s. Taking into account the matching of the carrier frequencies and wave vectors in the resonant triplet (polariton 1 — polariton 2 — LO phonon), we will treat the interacting macroscopic fields of Eqs. (4a)–(4e) in the following form ($j=1,2$):

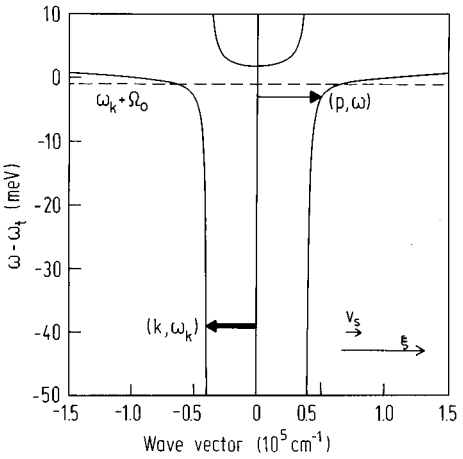

FIG. 1. Scheme of the resonant polariton-polariton Raman interaction. Polariton 1 — $(\mathbf{p},\omega)$; polariton 2 — $(\mathbf{k},\omega_{\mathbf{k}})$, $\mathbf{p}\|\mathbf{k}\|\boldsymbol{\xi}$ axis; v_s is the velocity of the coupled solitons. The following CdS parameters have been used in the calculations: $\hbar\omega_t=2.552$ eV, $\hbar\omega_{\perp t}=1.9$ meV, $\varepsilon_\infty=\varepsilon_g=9.3$, $m_e=0.2m_0$, $m_h=m_{h\perp}=0.7m_0$, $a_x=28$ Å, $\hbar\Omega_0=38$ meV, $\varepsilon_0=5.8$.

$$E_j^{(+)}(\xi,t)=\tilde{E}_j(\tau)\exp(-i\omega_j t+ip_j\xi),$$

$$P_j^{(+)}(\xi,t)=\tilde{P}_j(\tau)\exp(-i\omega_j t+ip_j\xi),$$

$$\Phi^{(+)}(\xi,t)=\tilde{\Phi}(\tau)\exp[-i(\omega_1-\omega_2)t+i(p_1-p_2)\xi]. \quad (6)$$

Here, $(p_1,\omega_1)=(p,\omega)$ for the first polariton and $(p_2,\omega_2)=(-k,\omega_{\mathbf{k}})$ for the second polariton, $\tau=t-\xi/v_s$ is the retarded time. The considered geometry of the RRI is shown schematically in Fig. 1. The positive (negative) sign of v_s corresponds to backward (forward) scattering, when the interacting coherent polaritons counterpropagate (copropagate).

In order to simplify the initial set of Eqs. (4a)–(4e), we use the slowly varying envelope approximation (SVEA) (see, e.g., Ref. 10). Within the SVEA Eqs. (4a)–(4e) reduce to the following set of the first order nonlinear differential equations:

$$-id_1\tilde{E}_1'+c_1\tilde{E}_1=i\delta_1\tilde{P}_1'+\gamma_1\tilde{P}_1, \quad (7a)$$

$$a_1\tilde{P}_1-ib_1\tilde{P}_1'=\nu\tilde{P}_2\tilde{\Phi}+i\sigma\tilde{P}_2\tilde{\Phi}'+\alpha\tilde{E}_1, \quad (7b)$$

$$a_{\mathrm{ph}}\tilde{\Phi}-ib_{\mathrm{ph}}\tilde{\Phi}'=\nu_{\mathrm{ph}}\tilde{P}_2^*\tilde{P}_1, \quad (7c)$$

$$-id_2\tilde{E}_2'+c_2\tilde{E}_2=i\delta_2\tilde{P}_2'+\gamma_2\tilde{P}_2, \quad (7d)$$

$$a_2\tilde{P}_2-ib_2\tilde{P}_2'=\nu\tilde{P}_1\tilde{\Phi}^*-i\sigma\tilde{P}_1(\tilde{\Phi}^*)'+\alpha\tilde{E}_2, \quad (7e)$$

where $\tilde{F}'\equiv d\tilde{F}/d\tau$ $(\tilde{F}=\tilde{E}_j,\tilde{P}_j,\tilde{\Phi})$ and the coefficients are given by

$$a_j=\omega_t^2-\omega_j^2+\frac{\hbar\omega_t}{M}p_j^2,\quad b_j=2\left[\omega_j+\frac{\hbar\omega_t}{v_sM}p_j\right],$$

$$c_j=p_j^2-\frac{\varepsilon_g}{c^2}\omega_j^2,\quad d_j=2\left[\frac{\varepsilon_g}{c^2}\omega_j+\frac{p_j}{v_s}\right],$$

$$\gamma_j=\frac{4\pi}{c^2}\omega_j^2,\quad \delta_j=\frac{8\pi}{c^2}\omega_j,$$

$$\alpha=\omega_t^2\widetilde{\beta}=\frac{\varepsilon_g}{4\pi}\Omega_c^2,\quad a_{\rm ph}=\Omega_0^2-(\omega-\omega_{\mathbf{k}})^2,$$

$$b_{\rm ph}=2(\omega-\omega_{\mathbf{k}}),\quad \nu_{\rm ph}=\frac{\mathscr{L}}{\omega_t\sqrt{\rho}}\widetilde{\beta},$$

$$\sigma=2\omega_t\sqrt{\rho}\mathscr{L}\frac{(p+k)}{v_s},\quad \nu=\omega_t\sqrt{\rho}\mathscr{L}(p+k)^2. \tag{8}$$

In the macroscopic equations, (7a)–(7e), both the exciton and LO-phonon incoherent scattering are neglected, i.e., $\Gamma^x=\Gamma^{\rm ph}=0$. Therefore, we analyze coherent three-wave interaction (polariton 1—polariton 2—coherent LO phonon), due to the conservative nonlinearity. This assumption is valid in the high-intensity limit for a hypertransient regime, when a characteristic duration τ_s of the LO-phonon–mediated polariton-polariton interaction is shorter than the coherence times, i.e., $\tau_s\leqslant\min\{(\Gamma^x/2)^{-1},(\Gamma^{\rm ph}/2)^{-1}\}$ at a given point ξ. Mathematically, the solitonlike solutions of the initial set of Eqs. (4a)–(4e) can exist only in this regime. In Sec. VII, we will discuss this assumption in more detail.

In the SVEA one can express, from Eqs. (7a) and (7d), the envelopes $\widetilde{E}_{j=1,2}$ of the electric fields through the envelopes $\widetilde{P}_{j=1,2}$ of the corresponding excitonic polarizations:

$$\widetilde{E}_j=\frac{\gamma_j}{c_j}\widetilde{P}_j+\frac{i}{c_j}\left[\delta_j+\frac{d_j\gamma_j}{c_j}\right]\widetilde{P}_j'. \tag{9}$$

Then, the substitution of Eq. (9) in Eqs. (7b) and (7e) reduces Eqs. (7a)–(7e) to

$$\widetilde{P}_1'=-iq_1\widetilde{P}_1-i\rho_1|\widetilde{P}_2|^2\widetilde{P}_1+i\beta_1\widetilde{P}_2\widetilde{\Phi}, \tag{10a}$$

$$\widetilde{\Phi}'=-iq_{\rm ph}\widetilde{\Phi}+i\beta_{\rm ph}\widetilde{P}_2^*\widetilde{P}_1, \tag{10b}$$

$$\widetilde{P}_2'=-iq_2\widetilde{P}_2-i\rho_2|\widetilde{P}_1|^2\widetilde{P}_2+i\beta_2\widetilde{P}_1\widetilde{\Phi}^*. \tag{10c}$$

The coefficients in Eqs. (10a)–(10c) are given by ($j=1,2$)

$$q_{\rm ph}=\frac{a_{\rm ph}}{b_{\rm ph}},\quad \beta_{\rm ph}=\frac{\nu_{\rm ph}}{b_{\rm ph}},\quad \Delta_j=b_j+\frac{\alpha}{c_j}\left[\delta_j+\frac{d_j\gamma_j}{c_j}\right],$$

$$\rho_j=\frac{\sigma\beta_{\rm ph}}{\Delta_j},\quad \beta_j=\frac{1}{\Delta_j}(\nu+\sigma q_{\rm ph}),\quad q_j=\frac{1}{\Delta_j}\left[a_j-\alpha\frac{\gamma_j}{c_j}\right]. \tag{11}$$

The closed set of the coupled nonlinear differential Eqs. (10a)–(10c) contains the coherent polarizations as the variables rather than the electromagnetic fields as it is usually supposed in nonlinear optics. The physical reason of this feature is that the phonon-mediated polariton-polariton interaction involves only the excitonic components. Moreover, within Eqs. (10a)–(10c), one avoids a treatment of the nonlinear optical processes by means of a perturbation theory. The analysis[11,14,15] of RRI of the intense polaritons shows that the corresponding total resonant susceptibility $\chi(p,\omega\simeq\omega_{\mathbf{k}}+\Omega_0,|\widetilde{E}_2|^2)$ or $\chi(k,\omega_{\mathbf{k}}\simeq\omega-\Omega_0,|\widetilde{E}_1|^2)$, for the first (second) polariton, contains an additional intensity-dependent term in its resonant *denominator* $\Delta\omega=\omega-\omega_{\mathbf{k}}-\Omega_0$. Consequently, one cannot expand the total susceptibility χ in a power series of $|\widetilde{E}_2|^2$ (or $|\widetilde{E}_1|^2$) near the pole $\Delta=0$ and keep only the lowest-order resonant optical susceptibilities $\chi^{(2)}$ and $\chi^{(3)}$. The treatment of the polarizations $\widetilde{P}_j$ rather than the electric fields $\widetilde{E}_j$ in Eqs. (10a)–(10c) deals with the *inverse* total susceptibility $\chi^{(-1)}$. Therefore, this approach includes, within the initial microscopic model of Eq. (1), a whole set $\{\chi^{(n)}\}$ and avoids an expansion of χ in a frequency vicinity of the pole $\Delta=0$.

The first term on the r.h.s. of Eqs. (10a) and (10c) describes the polariton effects. The condition $q_j=0$ ($j=1,2$) gives the polariton dispersion $\omega_j=\omega^{\rm pol}(p_j)$. The second term characterizes the coherent generation or decay of a given polariton in the Raman interaction of the LO phonon and conjugated polariton. The even-order Raman susceptibilities $\chi^{(2n)}$ are responsible for this process. The third term on the r.h.s. of Eqs. (10a) and (10c) results from a whole set of the odd-order susceptibilities $\chi^{(2n+1)}$ ($n\geqslant1$). One can also attribute this nonlinearity to the phonon-mediated polariton-polariton interaction. There is no phonon-mediated polariton self-interaction, because $M_{x\text{-ph}}(|\mathbf{p}-\mathbf{k}|=0)=0$, according to Eq. (3). The second term on the r.h.s. of the reduced LO-phonon wave equation (10b) describes a coherent phonon generation in the RRI of the two intense coherent polaritons.

The principal difference between the fundamental traveling Raman TWS's in molecular systems and in semiconductors is that the vibrations or rotations are located at molecules, while the bulk phonons are propagating modes with well-defined eigenwave vectors. Therefore, one can introduce an unique retarded time τ for the all components of the traveling Raman TWS's in a semiconductor. As a result, Eqs. (10a)–(10c) are the *ordinary* differential equations. In molecular optics, the fundamental TWS's can be modeled only within a set of the *partial* differential equations,[4–8] because there are two different times, i.e., a located time (or coordinate) for the vibrations or rotations and a retarded time for the two traveling optical fields.

Introducing the real amplitudes x_j, z and phases φ_j ($j=1,2$), ψ of the complex envelopes of the polarizations,

$$\widetilde{P}_j=x_je^{i\varphi_j},\quad \widetilde{\Phi}=ze^{i\psi}, \tag{12}$$

one obtains from Eqs. (10a)–(10c):

$$x_1'=\beta_1x_2z\sin\Theta, \tag{13a}$$

$$x_2'=-\beta_2x_1z\sin\Theta, \tag{13b}$$

$$z'=-\beta_{\rm ph}x_1x_2\sin\Theta, \tag{13c}$$

$$x_1\varphi_1'=-(q_1+\rho_1x_2^2)x_1+\beta_1x_2z\cos\Theta, \tag{13d}$$

$$x_2\varphi_2' = -(q_2+\rho_2 x_1^2)x_2+\beta_2 x_1 z\cos\Theta, \tag{13e}$$

$$z\psi' = -q_{\rm ph}z+\beta_{\rm ph}x_1x_2\cos\Theta. \tag{13f}$$

Here, $\Theta=\varphi_1-\varphi_2-\psi$ is the phase-matching angle for the interacting polarization waves.

The first three amplitude Eqs. (13a)–(13c) obey three Manley-Rowe relations:

$$\beta_2 x_1^2+\beta_1 x_2^2=C_1, \quad -\beta_{\rm ph}x_1^2+\beta_2 z^2=C_2,$$

$$\beta_{\rm ph}x_1^2+\beta_1 z^2=C_3, \tag{14}$$

where $C_{i=1,2,3}$ are the constants of the motion. Only two of these relationships are independent. The Manley-Rowe integrals of the motion are due to the conservative three-wave resonant interaction in our model. In the resonant nonlinear triplet of the fundamental TWS's, two of the nonlinear waves are solitary, i.e., their amplitudes vanish when $\tau\to\pm\infty$. Therefore, for the traveling fundamental solitons, at least one of the constants C_i in Eqs. (14) has to be zero.

If $C_1=0$, the coherent LO phonon is a nonlinear pump wave in the traveling soliton triplet. This case involves a preliminary resonant generation of the intense coherent cw LO phonon and can hardly be realized. The conditions $C_2=0$ or $C_3=0$ correspond to possible experimental situations, when the first or the second coherent polariton, respectively, acts as a nonlinear pump. However, the case $C_2=0$, when a pump polariton has the higher carrier frequency ω ($\omega>\omega_{\mathbf{k}}$), corresponds to unstable TWS's. The physical origin of this instability stems from the spontaneous Raman decay of the pump polariton **p** (polariton 1) into LO phonon $\mathbf{p}-\mathbf{k}$ and its Stokes component **k** (polariton 2). This instability leads to stimulated Raman scattering, which can end up in the formation of stable TWS's. However, the structure of these TWS's corresponds to a pump polariton at the Stokes frequency $\omega_{\mathbf{k}}$. Such a scenario is responsible for the generation of Raman solitons in para-H_2.[4–8] Therefore, we will analyze the most interesting and important case, when $C_3=0$ and the second lower-frequency polariton acts as a nonlinear pump (see Fig. 1).

For $C_3=0$, one obtains from Eqs. (14)

$$x_1^2=-\frac{\beta_1}{\beta_2}(x_{02}^2-x_2^2), \quad z^2=\frac{\beta_{\rm ph}}{\beta_2}(x_{02}^2-x_2^2), \tag{15}$$

where $x_{02}=\widetilde{P}_2(\tau\to\pm\infty)$ is the cw amplitude of the excitonic polarization of the pump polariton 2.

In accordance with Eqs. (8) and (11), the real parameter $\beta_{\rm ph}>0$. From Eqs. (15), one concludes that the final nonlinear solutions have to be consistent with the condition $\beta_1<0$, because $\beta_1/\beta_{\rm ph}=-x_1^2/z^2<0$. With Eqs. (15), Eqs. (13a)–(13f) reduce to the following coupled equations for the dimensionless amplitude $Y=x_2/x_{02}$ and the phase-matching angle Θ:

$$\dot{Y}=(1-Y^2)\sin\Theta, \quad \dot{\Theta}=\widetilde{B}+\left[\frac{1-Y^2}{Y}-2Y\right]\cos\Theta+\kappa Y^2, \tag{16}$$

where the parameters $\widetilde{B}$ and κ are given by

$$\widetilde{B}=\frac{\rho_1 x_{02}^2+q_{\rm ph}+q_2-q_1}{x_{02}\sqrt{(-\beta_1)\beta_{\rm ph}}}, \quad \kappa=-\frac{2\rho_1 x_{02}^2}{x_{02}\sqrt{(-\beta_1)\beta_{\rm ph}}}. \tag{17}$$

In Eqs. (16), the derivative $\dot{F}=dF/dT$ is taken with respect to the dimensionless time T:

$$T=\tau x_{02}\sqrt{(-\beta_1)\beta_{\rm ph}}. \tag{18}$$

Introducing dimensionless variables u and v by

$$u=Y\cos\Theta, \quad v=Y\sin\Theta, \tag{19}$$

the set of Eqs. (16) can be rewritten as

$$\dot{u}=2uv-\widetilde{B}v-\kappa v(u^2+v^2),$$

$$\dot{v}=1-3u^2-v^2+\widetilde{B}u+\kappa u(u^2+v^2). \tag{20}$$

One can treat u and v as the canonically conjugated variables and then construct formally a generating Hamiltonian for Eqs. (20):

$$H(u,v)=\left[\frac{\widetilde{B}}{2}+\frac{\kappa}{4}\right](u^2+v^2)-u(u^2+v^2-1). \tag{21}$$

$H(u,v)$ is an integral of the motion of Eqs. (20). The asymptotic stationary points of Eqs. (20), which characterize the coupled fundamental solitons at $\tau\to\pm\infty$, are given by

$$u_\infty=\frac{\widetilde{B}+\kappa}{2}, \quad v_\infty=\pm\left[1-\frac{(\widetilde{B}+\kappa)^2}{4}\right]^{1/2}. \tag{22}$$

Therefore, one finds the following algebraic relationship between u and v:

$$H(u,v)=H(u_\infty,v_\infty)=\frac{2\widetilde{B}+\kappa}{4}. \tag{23}$$

Using the integral of the motion (23) and Eqs. (15), one derives from Eqs. (20) and Eqs. (13a)–(13f) the intensity profiles z^2, $x_{j=1,2}^2$ and the phase-matching angle Θ of the fundamental traveling TWS's:

$$x_2^2=[1\mp\Phi_\pm(2\tau/\tau_s)]x_{02}^2, \quad x_1^2=\frac{(-\beta_1)}{(\mp\beta_2)}\Phi_\pm(2\tau/\tau_s)x_{02}^2,$$

$$z^2=\frac{\beta_{\rm ph}}{(\mp\beta_2)}\Phi_\pm(2\tau/\tau_s)x_{02}^2, \tag{24a}$$

$$\Theta=-\arctan\frac{2[(1-B^2/4)(\kappa^2+2B\kappa+4)]^{1/2}\sinh(2\tau/\tau_s)}{B(\kappa^2+2B\kappa+4)^{1/2}\cosh(2\tau/\tau_s)\pm 2(\kappa+B)}, \tag{24b}$$

where the function $\Phi_\pm(2\tau/\tau_s)$ and the coefficient B are given by

$$\Phi_\pm(2\tau/\tau_s)=\frac{4(1-B^2)}{(\kappa^2+2B\kappa+4)^{1/2}\cosh(2\tau/\tau_s)\pm(B\kappa/2+2)}, \tag{25}$$

$$B=-(\kappa+\widetilde{B}). \tag{26}$$

In Eqs. (24) and (25), we returned to the dimensional retarded time τ ($\tau=0$ refers to a center of the coupled solitons) and the characteristic soliton duration τ_s is

$$\tau_s=\left[x_{02}\sqrt{(-\beta_1)\beta_{\rm ph}}\left(1-\frac{B^2}{4}\right)^{1/2}\right]^{-1}. \tag{27}$$

According to Eqs. (24a), the two mutually coupled polariton 1 and coherent LO phonon are solitary waves, which have similar profiles $z^2(2\tau/\tau_s)=(\beta_{\rm ph}/(-\beta_1))x_1^2(2\tau/\tau_s)$. A kind of the Raman TWS's is determined by a sign of the parameter β_2. For $\beta_2<0$ [the upper sign in Eqs. (24) and (25)], the two coupled bright solitons ''burn'' a traveling steady-state dip in the cw intensity of the nonlinear polariton 2. The odd-order nonlinear susceptibilities $\chi^{(2n+1)}$ give $\kappa\neq 0$ and prevent a decrease of the amplitude of the nonlinear pump down to zero, even at the exact Raman resonance $\omega-\omega_{\mathbf{k}}=\Omega_0$. A finite amplitude of the dip at $\tau=0$ corresponds to the so-called gray soliton.[23] For $\kappa=0$, this gray soliton transforms to a dark one, which can be also interpreted as a kink structure in the cw complex amplitudes $\widetilde{P}_2$ and $\widetilde{E}_2$ of the second polariton. For $\beta_2>0$ [the lower sign in Eqs. (24) and (25)], the two coupled solitary waves form a spike in the cw intensity profile of the pump polariton 2, i.e., an antidark soliton according to the terminology of Ref. 23. Again, $\kappa\neq 0$ prevents an explosive instability,[24] when the denominators in Eqs. (24) and (25) are equal to zero at $\tau=0$ for $\omega-\omega_{\mathbf{k}}=\Omega_0$.

The fundamental solutions given by Eqs. (24a) and (24b) do not exhaust the description of the three-wave coupled solitons. According to Eqs. (8), (11), and (27), the carrier frequencies $\omega_{j=1,2}=(\omega,\omega_{\mathbf{k}})$, and wave vectors $p_{j=1,2}=(p,k)$ of the interacting polaritons, the characteristic soliton duration τ_s and velocity v_s, and the cw amplitude of the pump polariton 2 are involved as the seven parameters in Eqs. (24) and (25). However, not all of them are independent. E.g., Eq. (27) is one of the relationships between these parameters. The requirement of the absence of the phase modulation at $\tau\to\pm\infty$ (or $T\to\pm\infty$)

$$\varphi_1'|_{\tau\to\pm\infty}=\varphi_2'|_{\tau\to\pm\infty}=\zeta'|_{\tau\to\pm\infty}=0 \tag{28}$$

gives rise to other links between the initial parameters. Equations (28) imply a solitonlike behavior of the polarization phases φ, ψ, and ζ of the fundamental TWS's. From Eqs. (28), treating Eqs. (13d)–(13f) and (24b), one obtains the following additional relationships:

$$q_1+q_{\rm ph}=-\rho_1 x_{02}^2, \tag{29a}$$

$$q_2=0. \tag{29b}$$

Equations (29a) and (29b) are the dispersion equations for the first and second coupled nonlinear polaritons, respectively. From Eqs. (26), (29a), and (29b), one gets

$$B=-\frac{2q_{\rm ph}}{x_{02}\sqrt{(-\beta_1)\beta_{\rm ph}}}. \tag{30}$$

The further analysis depends on a selection of the four free parameters. We choose ω_j, $x_{02}=|\widetilde{P}_2(\tau\to\pm\infty)|$ and τ_s as the independent ones. Experimentally, such a parametrization implies that the polaritons 1 and 2 are induced by two optical pulses of given frequencies $\omega_1=\omega$ and $\omega_2=\omega_{\mathbf{k}}$. The optical pulse 2 with the frequency $\omega_2\simeq\omega_1-\Omega_0$ and the intensity $I_2=I_0$ has a duration $\tau^{(2)}\gg\tau_s$. This pulse generates the pump polariton 2. The intensity I_0 determines the cw polarization amplitude $x_{02}\propto\sqrt{I_0}$ by

$$x_{02}^2=I_0\frac{\Omega_c^4}{\omega_{\mathbf{k}}\omega_t(\omega_t-\omega_{\mathbf{k}})^2}\left(\frac{\varepsilon_g^{3/2}}{8\pi c}\right)\frac{n_x(\omega_{\mathbf{k}})}{[n_x(\omega_{\mathbf{k}})+1]^2}, \tag{31}$$

where the polariton refraction index $n_x(\omega_{\mathbf{k}})=\sqrt{\varepsilon_g[\omega_{lt}/(\omega_t-\omega_{\mathbf{k}})]}\simeq\sqrt{\varepsilon_g}$, because $\omega_t-\omega_{\mathbf{k}}\gg\omega_{lt}$ (see Fig. 1). In Eq. (31), the reflection from a crystal surface is included explicitly for normal incidence of the external optical pulses. The optical pulse 1 of the duration $\tau^{(1)}\ll\tau^{(2)}$ induces the solitary polariton 1, with $\tau_s\simeq\tau^{(1)}$, i.e., determines the soliton duration τ_s. In this picture, the coupled traveling solitons can be generated only during the finite time interval of the polariton 1–polariton 2 interaction, i.e., a steady-state perturbation (dip or spike) at the quasi-continuous-wave profile of the long pump pulse arises at its leading edge and disappears at its trailing edge. Therefore, we deal with ''transient solitons'' in the terminology of Ref. 7.

IV. CLASSIFICATION OF THE FUNDAMENTAL TRAVELING SOLITONS

After parametrization, one has to find, from Eqs. (27), (29a), and (29b), the other three parameters $p_{j=1,2}=(p,k)$ and v_s. The dispersion Eq. (29b) determines the carrier wave vector $k=k(\omega_{\mathbf{k}})$ of the pump polariton 2 and reduces to the usual polariton dispersion:

$$a_2c_2-\alpha\gamma_2=\left(\omega_t^2-\omega_{\mathbf{k}}^2+\frac{\hbar\omega_t}{M}k^2\right)\left(k^2-\frac{\varepsilon_g}{c^2}\omega_{\mathbf{k}}^2\right)-\frac{\varepsilon_g}{c^2}\omega_{\mathbf{k}}^2\Omega_c^2=0. \tag{32}$$

This dispersion corresponds to a free propagation of the pump polariton 2 in the absence of the coupled solitary pulses, i.e., if $|\tau|\gg\tau_s$.

Equations (27) and (29a) are a closed set of algebraic equations for the soliton velocity $v_s=v_s(\omega,\omega_{\mathbf{k}},x_{02},\tau_s)$ and the carrier wave vector $p=p(\omega,\omega_{\mathbf{k}},x_{02},\tau_s)$ of the solitary polariton 1. This set reduces to an algebraic dispersion equation of ninth order for the wave vector p. We study numerically this equation in order to find the real roots p, which correspond to the traveling nonlinear waves of Eqs. (6). All the numerical calculations in our work are given for a CdS crystal. The typical dispersion $p=p(\omega,\omega_{\mathbf{k}},x_{02},\tau_s)$ for the given values of $\omega_{\mathbf{k}}$, I_0, (or x_{02}) and τ_s is shown in Fig. 2. We classify the fundamental traveling TWS's according to the dispersion of the solitary polariton 1.

The various dispersion branches 1–6 (see Fig. 2) for the solitary polariton 1 stem from mutual hybridization and splitting of the initial LO phonon (dashed line in Fig. 2) and polariton dispersions in the presence of a nonlinear pump polariton 2. This strong spectral modification occurs in a spectral vicinity of the anti-Stokes resonance of the pump polariton, i.e., when $\omega\simeq\omega_{\mathbf{k}}+\Omega_0$, and gives rise to the closed dispersion curves 4–5 and to the dispersion anomalies in the branches 1–3. With decreasing pump intensity I_0 (pa-

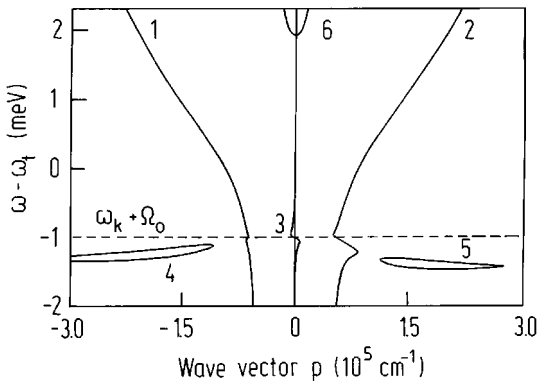

FIG. 2. The nonlinear dispersion $p=p(\omega)$ of the solitary polariton 1, $\hbar\omega_{\mathbf{k}}=2.513$ eV $[\hbar(\omega_t-\omega_{\mathbf{k}}-\Omega_0)=1$ meV], $I_0=500$ MW/cm^2, $\tau_s=15$ ps; 1–2 — the dispersion branches of the quasipolariton TWS's; 3–5 — the dispersion branches of the quasiphonon TWS's, 6 — the upper polariton dispersion branch.

rameter x_{02}), the spectral regions of anomalous slope of the branches 1 and 2 decrease and these dispersion curves evolve continuously to the unperturbed lower polariton branches. The spectral curve 6 is the upper polariton branch. If the dispersion of the solitary polariton 1 in the soliton triplet is given by the branch 1 or 2, we will attribute these traveling fundamental TWS's to coupled *quasipolariton* solitons. The second class of the TWS's, which we will call *quasiphonon* solitons, refers to the dispersion branches 3–5. In a sense, these dispersion branches are the ''topological fragments'' of the LO-phonon dispersion. The closed curves 4 and 5, which resemble spectral ''droplets,'' disappear with decreasing pump intensity I_0.

The complicated dispersion for the bright polariton soliton 1 is similar to the phonoriton dispersion,[11,14,15] which describes a transient modification of the exciton, photon, and LO-phonon spectra of a semiconductor in the presence of a quasistationary coherent pump polariton 2. However, in this case, the first polariton is so weak ($I_1 \ll I_2=I_0$) that it does not disturb the cw profile of the pump polariton. The weak probe polariton 1 only tests the phonoriton dispersion, which is given by

$$\left(\omega_t^2-\omega^2+\frac{\hbar\omega_t}{M}p^2\right)\left(p^2-\frac{\varepsilon_g}{c^2}\omega^2\right)[(\omega-\omega_{\mathbf{k}})^2-\Omega_0^2] - \frac{16\pi\omega_t^2\mathscr{S}^2}{\varepsilon_g\Omega_c^2}x_{02}^2(p-k)^2\left(p^2-\frac{\varepsilon_g}{c^2}\omega^2\right) - \frac{\varepsilon_g}{c^2}\omega^2\Omega_c^2[(\omega-\omega_{\mathbf{k}})^2-\Omega_0^2]=0. \tag{33}$$

The dispersion Eq. (33) is analyzed in detail in Ref. 15. Physically, both the phonoriton dispersion Eq. (33) and the dispersion of the solitary polariton 1, Eqs. (27) and (29a), originate from the coherent phonon-mediated resonant oscillations between the polaritons 1 and 2.

Equations (27) and (29a) show that for given I_0 and $\omega_{\mathbf{k}}$ the dispersion of the solitary polariton 1 coincides with the corresponding phonoriton dispersion provided that

$$q_{\mathrm{ph}}^2\tau_s^2 \gg 1, \tag{34a}$$

$$\tfrac{1}{2}v_s(p+k)q_{\mathrm{ph}}\tau_s^2 \gg 1. \tag{34b}$$

The inequalities (34a) and (34b) hold for the upper sectors of the spectral droplets 4–5 and for the anomalous dispersion of the branch 3. These sectors coincide with the LO-phonon-like phonoriton branches (see Ref. 15). The phonoriton dynamical modification of the initial LO-phonon term is accompanied by a finite LO-phonon effective mass,[15] because $|M_{x-\mathrm{ph}}(p-k)|^2\propto(p-k)^2$ [see Eq. (1)]. The finite pump-induced LO-phonon effective mass has a negative sign and is $\propto I_0$. This result explains why the spectral droplets 4–5 appear below the unperturbed LO-phonon dispersion (dashed line in Fig. 2). The spectral range of validity of the inequalities (34a) and (34b) increases with the soliton duration τ_s. The regions of anomalous dispersion of the branches 1–3 and the lengths of the spectral droplets 4–5 also increase with increase of τ_s. Numerical calculations confirm these conclusions.

Along a given dispersion branch, the soliton velocity v_s has a definite sign. On the dispersion branches 1, 3, and 5, the velocity $v_s<0$, while along the curves 2 and 4, $v_s>0$. All of our numerical simulations justify this conclusion, although we have failed to prove it analytically. The sign of v_s determines a geometry of interaction of the first and second polaritons. Backscattering configuration corresponds to $v_s>0$, the initally generated polariton 1 and polariton 2 propagate in the opposite directions. In the forward scattering geometry $v_s<0$. For the spectral droplets 4, 5 and for the right part ($p>0$, see Fig. 2) of the quasiphonon branch 3, the carrier wave vector p of the solitary polariton 1 and its soliton velocity v_s have the opposite signs.

The quasiphonon TWS's cannot be obtained within the standard perturbation approach, which deals with the lowest nonlinear susceptibility $\chi^{(2)}$.[10] A dispersion of the Raman solitons in molecular optics is also considered as unperturbed or slightly perturbed.[4–8] In our case only, the quasipolariton dispersions 1 and 2 can be obtained by the continuous deformations of the unperturbed polariton branches.

V. QUASIPOLARITON SOLITONS

According to numerical simulations, at the quasipolariton dispersion branch 1, the parameter $\beta_2=\beta_2(\omega,\omega_{\mathbf{k}},I_0,\tau_s)<0$ in Eqs. (13a)–(13f) and the corresponding fundamental TWS's are given by Eqs. (24a) and (24b) with the upper sign. For the quasipolariton branch 2 $\beta_2>0$, thus one has to use the lower sign in Eqs. (24a) and (24b). Therefore, the kind of fundamental nonlinear pump polariton 2 in the quasipolariton TWS's depends on the interaction configuration, i.e., a gray soliton occurs in the forwardscattering geometry (branch 1) and an antidark soliton in the backscattering geometry (branch 2). This result is due to the strong dependence (3) of the $\mathscr{T}$ matrix element $M_{x-\mathrm{ph}}$ on the LO-phonon wave vector $\mathbf{p}-\mathbf{k}$. Typical amplitude profiles of the two coupled nonlinear polaritons of the quasipolariton TWS's calculated with Eqs. (24a) and (24b) and (29a) and (29b) are shown in Figs. 3(a) and 3(b) [see also Fig. 8(b)]. Both of the pairs of the coupled solitons of Figs. 3(a) and 3(b) (see the solid and dashed lines) have the same group velocity v_s. In accordance with Eqs. (24a), (24b), and (27), for fixed $\omega_{\mathbf{k}}$,

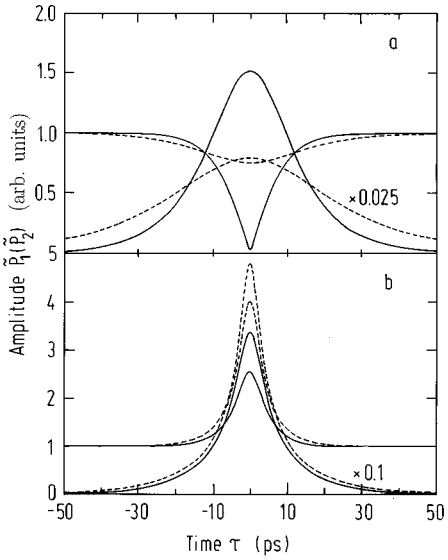

FIG. 3. Quasipolariton TWS's. The amplitude profiles $x_1=|\widetilde{P}_1(\tau)|$ and $x_2=|\widetilde{P}_2(\tau)|$ of the coupled nonlinear polaritons 1 and 2, respectively: (a) forward scattering (the dispersion branch 1); (b) backscattering (the dispersion branch 2). $I_0=50$ MW/cm^2, $\hbar\omega_{\mathbf{k}}=2.511$ eV $[\hbar(\omega_t-\omega_{\mathbf{k}}-\Omega_0)=3$ meV$]$, the soliton velocity $v_s=0.49\times10^{-2}$ $(c/\varepsilon_g^{1/2})$ are the same for all the plotted coupled solitons. The exact Raman resonance $\Delta\omega=0$ — solid lines $(\tau_s=10.0$ ps); the detuning $\hbar\Delta\omega=\hbar(\omega-\omega_{\mathbf{k}}-\Omega_0)=-0.04$ meV — dashed lines $[\tau_s=19.3$ ps for forward scattering (a) and $\tau_s=12.0$ ps for backscattering (b)$]$.

x_{02}, and v_s, the TWS's have a minimum duration at the exact Raman resonance $\omega=\omega_{\mathbf{k}}+\Omega_0$ $(B=0)$. Such a behavior is clearly seen in Figs. 3(a) and 3(b).

According to Eqs. (22) and (26), the coordinate v_∞ of the asymptotic stationary points will be real provided that $|B|\leqslant 2$. With Eq. (30), this condition reduces to

$$|q_{\rm ph}|\simeq|\omega-\omega_{\mathbf{k}}-\Omega_0|\leqslant x_{02}\sqrt{(-\beta_1)\beta_{\rm ph}}. \tag{35}$$

For the considered parametrization $(\omega_{j=1,2},\ x_{02},\ \tau_s)$, the inequality (35) holds, due to Eq. (27) for arbitrary detuning $\Delta\omega=\omega-\omega_{\mathbf{k}}-\Omega_0$ from the exact Raman resonance. However, the best-developed quasipolariton TWS's occur for $\Delta\omega=0$. The dimensionless detuning is given by the parameter $B\propto(\omega-\omega_{\mathbf{k}}-\Omega_0)$ of Eq. (30).

Typical quasipolariton soliton envelopes of the polarization phases $\varphi_j=\varphi_j(\tau)$, $\psi=\psi(\tau)$, and the corresponding phase-matching angle $\Theta=\Theta(\tau)$ are shown in Fig. 4 (the solid and dashed lines, respectively) for the backscattering interaction at the exact Raman resonance $\Delta\omega=0$ $(B=0)$. For the quasipolariton TWS's, $\Delta\Theta=\Theta(\tau\to+\infty)-\Theta(\tau\to-\infty)=\pi$ if $\Delta\omega=0$. This is an unique behavior for the Raman TWS's.[4–8] The π jump initiates a constructive change of stimulated inverse scattering on the normal one. However, in our case the π jump of the phase-matching angle Θ occurs for the polarization envelopes rather than for the electric fields.

From Eqs. (24a), one concludes that the solitary polariton 1 is a giant parametric pulse in the soliton triplet, because for the quasipolariton TWS's $K=x_1^{\max}(\tau=0)/x_{02}=|\widetilde{P}_1(\tau=0)|/|\widetilde{P}_2(\tau\to\pm\infty)|\gg1$, both for backscattering and forward scattering. The dependences $K=K(I_0)$, for the several values of τ_s, are shown in Fig. 5 ($K=K_b$ for backscattering and $K=K_f$ for forward scattering).

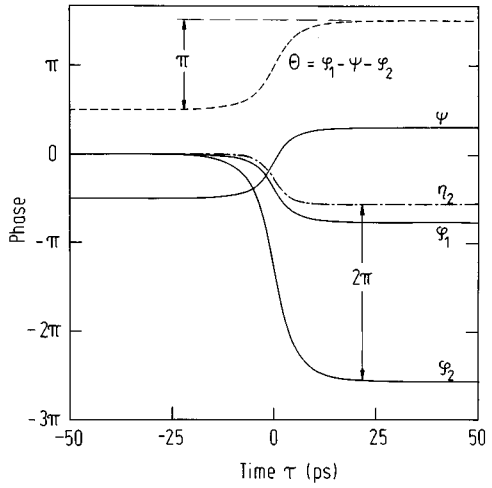

FIG. 4. Quasipolariton TWS's, backscattering polariton-polariton interaction (the dispersion branch *2*). The soliton envelopes $\varphi_{1,2}=\varphi_{1,2}(\tau)$, $\psi=\psi(\tau)$ (solid lines), and the phase-matching angle $\Theta=\Theta(\tau)$ (dashed line). $I_0=50$ MW/cm^2, $\hbar\omega_{\mathbf{k}}=2.511$ eV $[\hbar(\omega_t-\omega_{\mathbf{k}}-\Omega_0)=3$ meV$]$, $\tau_s=10$ ps, the exact Raman resonance $\Delta\omega=0$ (the corresponding amplitude profiles are shown in Fig. 3(b) by the solid lines). The soliton envelope of the phase $\eta_2=\eta_2(\tau)$ of the electric field $\widetilde{E}_2=y_2e^{i\eta_2}$ of the pump polariton 2 (dash-dotted line).

The dependences of the soliton velocity $v_s=v_s(\omega)$ for given $\omega_{\mathbf{k}}$, τ_s and two values of the pump intensity I_0 are shown in Fig. 6, both for the forward scattering and backscattering polariton-polariton interactions. According to

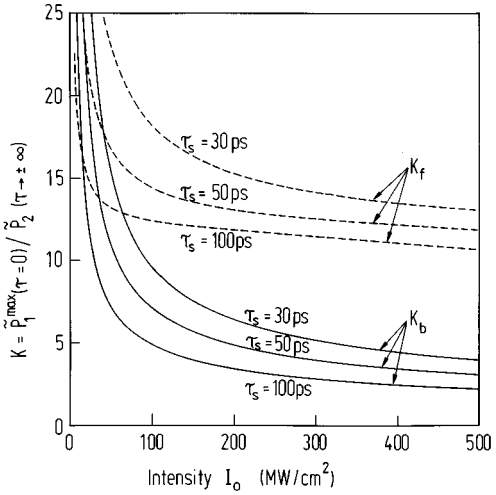

FIG. 5. Quasipolariton TWS's. The maximum amplitude $x_1^{\max}(\tau=0)$ of the giant parametric solitary polariton 1 normalized to the cw amplitude x_{02} of the polariton 2 versus intensity I_0. Solid lines — the backscattering geometry (the dispersion branch *2*, $K=K_b$); dashed lines — the forward scattering geometry (the dispersion branch *1*, $K=K_f$); $\hbar\omega_{\mathbf{k}}=2.511$ eV $[\hbar(\omega_t-\omega_{\mathbf{k}}-\Omega_0)=3$ meV$]$, the exact Raman resonance $\Delta\omega=0$.

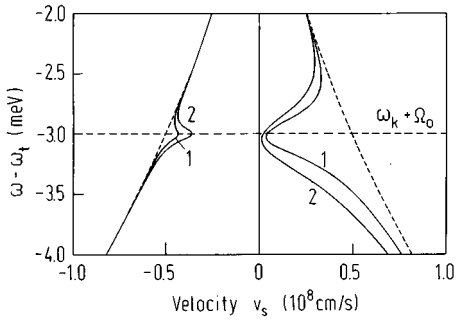

FIG. 6. Quasipolariton TWS's. The dependences of the soliton velocity $v_s = v_s(\omega)$ (solid lines) for $\hbar\omega_{\mathbf{k}} = 2.511$ eV $[\hbar(\omega_t - \omega_{\mathbf{k}} - \Omega_0) = 3$ meV], $\tau_s = 10$ ps, and (1) $I_0 = 200$ MW/cm^2, (2) $I_0 = 500$ MW/cm^2 (the left part — forward scattering; the right part — backscattering). Dashed lines indicate the unperturbed polariton group velocity $v_{\mathrm{pol}} = v_{\mathrm{pol}}(\omega)$.

these graphs, the soliton velocity v_s has a minimum at the exact Raman resonance; with increasing detuning $\Delta\omega$, the soliton velocity $v_s(\omega)$ approaches the polariton group velocity $v_{\mathrm{pol}} = \partial\omega_{\mathrm{pol}}(p)/\partial p|_{p=p(\omega)}$ (dashed lines in Fig. 6), where $\omega_{\mathrm{pol}}(p)$ is the unperturbed polariton dispersion. The soliton velocity v_s of the quasipolariton TWS's decreases with intensity I_0 of the pump polariton 2 and is always less than the corresponding v_{pol}. Such a behavior of v_s is due to an increase of the LO-phonon component in the soliton triplet, with increasing I_0 or decreasing $|\Delta\omega|$. This LO-phonon component ''slows down'' the soliton propagation, because for the unperturbed LO-phonon dispersion $v_{\mathrm{LO}} = \partial\Omega_0/\partial p|_{p\to 0} = 0$.

VI. QUASIPHONON SOLITONS

The initial set of the macroscopic Eqs. (4a)–(4e) reduces to Eqs. (13a)–(13f) under the conditions:

$$v_s \gg \frac{c}{2\omega_t\tau_s\sqrt{\varepsilon_g}}, \tag{36a}$$

$$\tau_s\left|p^2 - \frac{\varepsilon_g}{c^2}\omega^2\right| \gg 2\left|\frac{\varepsilon_g}{c^2}\omega - \frac{p}{v_s}\right|, \tag{36b}$$

$$\tau_s\left|k^2 - \frac{\varepsilon_g}{c^2}\omega_{\mathbf{k}}^2\right| \gg 2\left|\frac{\varepsilon_g}{c^2}\omega_{\mathbf{k}} + \frac{k}{v_s}\right|, \tag{36c}$$

The inequality (36a) allows the SVEA. Equation (9), which gives the electric component of a polariton through its polarization component, are derived under the conditons (36b) and (36c) for the first and second polaritons, respectively. The validity of Eqs. (36a)–(36c) depends strongly on which dispersion branch they are tested. This dependence stems mainly from a value of the soliton velocity v_s in Eqs. (36a)–(36c).

Along the quasipolariton dispersion branches 1 and 2, Eqs. (36a)–(36c) hold provided that the cw intensity of the pump polariton 2 is not too high $I_0 \leqslant 1$GW/cm^2. The conditions (36b) and (36c) imply that on the r.h.s. of Eqs. (9) the second term is considerably smaller than the first one. This denotes a slightly perturbed internal polariton structure of the both coupled polariton solitons, because for a free linear polariton $\tilde{E}_j = (\gamma_j/c_j)\tilde{P}_j$ [see Eqs. (9)]. In other words, for the quasipolariton TWS's the LO-phonon – mediated polariton-polariton interaction does not destroy the balance between exciton and photon components in the first and second polaritons.

For the quasiphonon Raman TWS's, i.e., along the dispersion branches 3–5, Eqs. (36a) and (36b) are satisfied only for $I_0 \geqslant I_{\mathrm{th}}^{(1)}(\tau_s)$, while Eq. (36c) is always broken, due to the small values of the soliton velocity v_s. The threshold intensity $I_{\mathrm{th}}^{(1)}(\tau_s)$ decreases with increasing soliton duration τ_s and is about 100–200 MW/cm^2 for $\tau_s = 15$ ps. If Eq. (9) does not hold for the pump polariton $j = 2$ of the quasiphonon TWS's, one has to describe explicitly the polarization $\tilde{P}_2$ and electric field $\tilde{E}_2$. Therefore, in the set of Eqs. (10a)–(10c), one has to treat Eqs. (7d) and (7e) instead of Eq. (10c). Introducing the real amplitudes and phases for all the polarization fields by Eqs. (12) and for the electric field $\tilde{E}_2 = y_2 e^{\eta_2}$, one can rewrite this generalized set in the following form:

$$x_1' = \beta_1 x_2 z \sin\Theta, \tag{37a}$$

$$x_2' = \frac{\alpha}{b_2} y_2 \sin\Lambda - \tilde{\beta}_2 x_1 z \sin\Theta, \tag{37b}$$

$$z' = -\beta_{\mathrm{ph}} x_1 x_2 \sin\Theta, \tag{37c}$$

$$d_2 y_2' = -\gamma_2 x_2 \sin\Lambda - \delta_2 x_2' \cos\Lambda + \delta_2 \varphi_2' x_2 \sin\Lambda, \tag{37d}$$

$$x_1\varphi_1' = -(q_1 + \rho_1 x_2^2)x_1 + \beta_1 x_2 z \cos\Theta, \tag{37e}$$

$$x_2\varphi_2' = -(\tilde{q}_2 + \tilde{\rho}_2 x_1^2)x_2 + \frac{\alpha}{b_2} y_2 \cos\Lambda + \tilde{\beta}_2 x_1 z \cos\Theta, \tag{37f}$$

$$z\psi' = -q_{\mathrm{ph}} z + \beta_{\mathrm{ph}} x_1 x_2 \cos\Theta; \tag{37g}$$

$$d_2 y_2 \eta_2' = -c_2 y_2 + \gamma_2 x_2 \cos\Lambda - \delta_2 x_2' \sin\Lambda + \delta_2 x_2 \varphi_2' \cos\Lambda. \tag{37h}$$

Here, $\Lambda = \varphi_2 - \eta_2$ and in addition to the notations given by Eqs. (8) and (11),

$$\tilde{q}_2 = \frac{a_2}{b_2}, \quad \tilde{\rho}_2 = \frac{\sigma\beta_{\mathrm{ph}}}{b_2}, \quad \tilde{\beta}_2 = \frac{\nu + \sigma q_{\mathrm{ph}}}{b_2}. \tag{38}$$

For the set of Eqs. (37a)–(37h), only the last Manley-Rowe relation of Eqs. (14) is preserved in the same form with $C_3 = 0$. Thus, in accordance with Eq. (15), the coupled solitary LO phonon and polariton 1 have again similar amplitude envelopes for the quasiphonon TWS's. For a numerical evaluation of the traveling fundamental quasiphonon TWS's within Eqs. (37a)–(37h), one has to find at first the corresponding asymptotic stationary points. These points of Eqs. (37a)–(37h) are given by

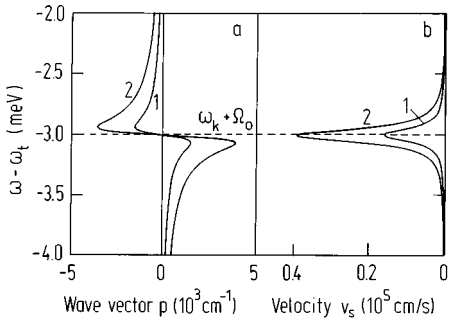

FIG. 7. Quasiphonon TWS's. (a) The magnified region of the quasiphonon dispersion branch 3, (b) the corresponding soliton velocity $v_s=v_s(\omega)$; $\hbar\omega_{\mathbf{k}}=2.511$ eV $[\hbar(\omega_t-\omega_{\mathbf{k}}-\Omega_0)=3$ meV], $\tau_s=15$ ps, and (1) $I_0=200$ MW/cm^2, (2) $I_0=500$ MW/cm^2.

$$x_{1\infty}=0,\quad z_{1\infty}=0,\quad x_{2\infty}=x_{02},\quad y_{2\infty}=y_{02}=\frac{a_2}{\alpha}x_{02},$$

$$\Lambda_\infty=\varphi_{2\infty}-\eta_{2\infty}=0,\quad \cos\Theta_\infty=\frac{q_{\rm ph}}{x_{02}\sqrt{(-\beta_1)\beta_{\rm ph}}}=-\frac{B}{2}. \tag{39}$$

The conditions (28) for the set of Eqs. (37a)–(37h) result again in the dispersion Eqs. (29a) and (29b). In order to find the soliton characteristic duration τ_s, one can treat analytically the asymptotic behavior of the soliton solutions of Eqs. (37a)–(37h) at $\tau\to\pm\infty$, i.e. in a vicinity of the stationary points given by Eq. (39). Linearization of Eqs. (37a)–(37h) around these points yields the exponential envelopes of the solitary waves at $\tau\to\pm\infty$:

$$x_1(\tau\to\pm\infty)=X_0\exp(\mp\tau/\tau_s),$$

$$z(\tau\to\pm\infty)=Z_0\exp(\mp\tau/\tau_s), \tag{40}$$

where X_0 and Z_0 are the constants and the characteristic duration τ_s is again given by Eq. (27). *Therefore, all the relationships between the initial parameters, i.e., Eqs. (27) and (29a) and (29b), are preserved for the generalized set of Eqs. (37a)–(37h).*

The quasiphonon dispersion droplets 4 and 5 (see Fig. 2) disappear with decreasing I_0. Branch 5 always disappears first, e.g., for $\hbar\omega_{\mathbf{k}}=2.513$ eV and $\tau_s=15$ ps, both spectral droplets 4 and 5 exist for $I_0\geqslant 350$ MW/cm^2, for 350 MW/cm$^2\geqslant I_0\geqslant 200$ MW/cm^2 only spectral droplet 5 occurs, and for $I_0\leqslant 200$ MW/cm^2 there are no spectral droplets. We will concentate mainly on the the central quasiphonon dispersion branch 3. This dispersion is shown in detail in Fig. 7(a) for two values of I_0. The region of anomalous dispersion with negative slope increases with the intensity of the pump polariton 2. This anomalous dispersion can be treated as a slightly deformed sector of the unperturbed LO-phonon dispersion $\omega_{\mathbf{k}}+\Omega_0$ [dashed line in Fig. 7(a)].

The corresponding dependences of the soliton velocity $v_s=v_s(\omega)$ are presented in Fig. 7(b). The velocity v_s of the quasiphonon TWS's is anomalously small [$v_s\leqslant 10^5$ cm/s in Fig. 7(b)], increases with pump intensity I_0, and has a maximum value at the exact Raman resonance $\omega=\omega_{\mathbf{k}}+\Omega_0$ ($\Delta\omega=0$). For $\Delta\omega=0$, one gets from the dispersion Eq. (29a):

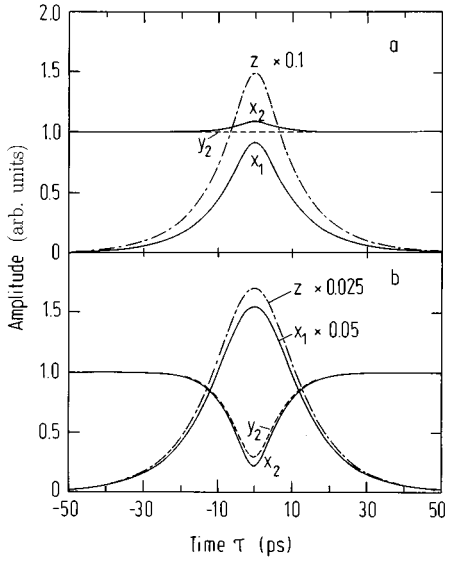

FIG. 8. Quasiphonon and quasipolariton TWS's in the forward-scattering geometry ($v_s<0$). The amplitude profiles $x_1=|\widetilde{P}_1(\tau)|$, $x_2=|\widetilde{P}_2(\tau)|$, $y_2=|\widetilde{E}_2(\tau)|$, and $z=|\widetilde{\Phi}(\tau)|$ of the coupled resonant triplet: (a) the quasiphonon TWS's of the dispersion branch 3, (b) the quasipolariton TWS's of the dispersion branch 1. The exact Raman resonance ($\Delta\omega=0$), $I_0=200$ MW/cm^2, $\hbar\omega_{\mathbf{k}}=2.512$ eV $[\hbar(\omega_t-\omega_{\mathbf{k}}-\Omega_0)=2$ meV], and $\tau_s=10$ ps.

$$v_s(\omega=\omega_{\mathbf{k}}+\Omega_0)=-\frac{x_{02}^2\mathscr{L}^2k}{\Omega_0\widetilde{\beta}(\omega_l^2-\omega^2)}\propto I_0, \tag{41}$$

where $\omega_l=\omega_t+\omega_{lt}$ is the frequency of the longitudinal exciton, the parameters $\mathscr{L}$ and $\widetilde{\beta}$ are defined by Eq. (3) and Eqs. (2), respectively. Equation (41) is derived under the conditions $|\omega_l-\omega|\gg\hbar k^2/M$ and $p\ll k$. These conditions hold for the quasiphonon TWS's, because for branch 3 the exact Raman resonance $\Delta\omega=0$ corresponds to $p=0$.

Typical amplitude envelopes $x_1(\tau)$, $x_2(\tau)$, $y_2(\tau)$, and $z(\tau)$ of the traveling fundamental quasiphonon TWS's, according to Eqs. (37a)–(37h), are shown in Fig. 8(a). For comparison, the corresponding envelopes for the quasipolariton TWS's of branch 1 are also shown in Fig. 8(b). The amplitude envelope $y_2(\tau)$ of the electric field of the pump polariton 2 is normalized to $y_{2\infty}=y_{02}$. The set of Eqs. (13a)–(13f) together with Eqs. (9) give the same envelopes for the quasipolariton solitons as the generalized set of Eqs. (37a)–(37h). Figure 8(b) with $y_2=y_2(\tau)$ very similar to $x_2=x_2(\tau)$ clearly indicates that, for the quasipolariton TWS's, the LO-phonon–mediated polariton-polariton interaction does not disturb the internal polariton structure of the pump. Both TWS's of Figs. 8(a) and 8(b), quasiphonon and quasipolariton, can be generated simultaneously in the forward scattering configuration ($v_s<0$).

According to Figs. 8(a) and 8(b), the ratio $z^{\max}/x_1^{\max}$ of the maximum amplitudes $z^{\max}=z(\tau=0)$ and $x_1^{\max}=x_1(\tau=0)$ of the coupled solitary LO phonon and polariton 1 is considerably larger for the quasiphonon TWS's. Thus, the quasiphonon TWS's are accompanied by a giant coherent LO phonon. On the other hand, the solitary polariton 1 of the

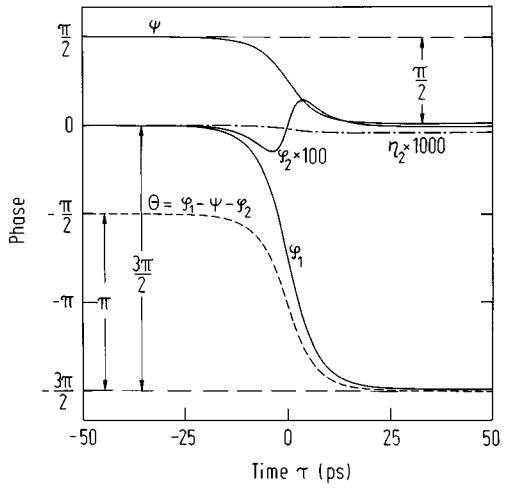

FIG. 9. Quasiphonon TWS's of the dispersion branch 3 (see Fig. 2). The soliton envelopes of the phases $\eta_2=\eta_2(\tau)$ (dash-dotted line), $\varphi_{1,2}=\varphi_{1,2}(\tau)$, $\psi=\psi(\tau)$ (solid lines), and the corresponding phase-matching angle $\Theta=\Theta(\tau)$ (dashed line). The exact Raman resonance $\Delta\omega=0$, $I_0=200$ MW/cm^2, $\hbar\omega_{\mathbf{k}}=2.511$ eV $[\hbar(\omega_t-\omega_{\mathbf{k}}-\Omega_0)=3$ meV], and $\tau_s=10$ ps.

quasiphonon TWS's has a maximum amplitude $x_1^{\max}$ of the same order as x_{02} [see Fig. 8(a)] and cannot be considered as a giant parametric pulse. Typical quasiphonon soliton envelopes of the phases $\varphi_j=\varphi_j(\tau)$ $(j=1,2)$, $\psi=\psi(\tau)$, and the corresponding phase-matching angle $\Theta=\Theta(\tau)$ are shown in Fig. 9 for branch 3 under exact Raman resonance condition $\Delta\omega=0$. The phase-matching angle Θ of the polarization phases again undergoes a π jump. However, the sign of this jump is opposite to that of the quasipolariton TWS's (see Fig. 4). This $-\pi$ jump of $\Theta=\varphi_1-\varphi_2-\psi$ for the quasiphonon TWS's follows the $-\pi/2$ jump of the coherent phonon phase ψ and the $-3\pi/2$ jump of the polarization phase φ_1 of the solitary polariton 1 (see Fig. 9).

According to the numerical simulations, the quasiphonon TWS's have extremely small variations of the amplitude $y_2(\tau)$ [see Fig. 8(a)] and the phase η_2 (see Fig. 9) of the electric field $\tilde{E}_2$ of the pump polariton 2:

$$y_2(\tau)/y_{02}\ll 1, \quad |\eta_2(\tau)-\eta_2(\tau\rightarrow\pm\infty)|\leqslant 0.001 \text{ rad}. \tag{42}$$

Equations (42) are derived from Eqs. (37d) and (37h) under the condition

$$\frac{\sqrt{\varepsilon_g}}{4}\frac{v_s\tau_s\Omega_c^2}{c\Omega_0}\ll 1. \tag{43}$$

The inequality (43) holds, due to the anomalously small v_s of the quasihonon TWS's. This result shows that generation of the quasiphonon TWS's cannot be observed in the cw background of the pump pulse (polariton 2), because only the electromagnetic component of a polariton is observable. Figure 9 shows also a small variation of the polarization phase ζ of polariton 2.

The extremely small velocity v_s of the quasiphonon TWS's stems from the large LO-phonon contribution Φ to these coupled solitons. Such a structure of the quasiphonon TWS's originates from the large differences between the branches 3–5 and the unperturbed polariton dispersion (see Fig. 2). Both the quasipolariton and the quasiphonon TWS's propagate only due to their photon and exciton components, because the unperturbed LO-phonon group velocity $v_{\mathrm{LO}}=0$. Contrary to the quasipolariton TWS's, the admixture of the photon and exciton components of the quasiphonon Raman solitons increases with the intensity I_0 of the pump polariton 2 resulting in the increase of v_s. If the condition (36c) becomes invalid, a strong perturbation of the polariton internal structure $[y_2/x_2=y_{02}/x_{02}\simeq a_2/\alpha=\gamma_2/c_2$ — see Eq. (32)] of the pump polariton 2 occurs in the presence of the coupled solitary LO phonon and polariton 1, i.e., in the region of the polariton-polariton Raman interaction. Therefore, the quasiphonon Raman TWS's can be understood as *four* coupled nonlinear fields: exciton P_2 and photon E_2 of the polariton 2, polariton 1 with the unperturbed internal structure $(c_1E_1=\gamma_1P_1)$, and coherent phonon Φ.

VII. DISCUSSION

The stability against small amplitude or phase perturbations is crucial for fundamental solitons. In order to examine this property for the quasiphonon TWS's, we linearize Eqs. (37a)–(37h) around the corresponding soliton solutions. After linearization, Eqs. (37a)–(37h) decouple into the two independent subsets of Eqs. (37a), (37c), (37e), (37g) and Eqs. (37b), (37d), (37f), (37h), respectively. The first one deals with the perturbations δx_1, δz, $\delta\varphi_1$, and $\delta\psi$. The corresponding linear solutions $\propto\exp(\delta\Omega_1 t)$ are stable, i.e., $\mathrm{Re}\{\delta\Omega_1\}<0$. The second set for δx_2, δy_2, $\delta\varphi_2$, and $\delta\eta_2$ gives

$$\delta\Omega_2=-\frac{i}{d_2b_2}(a_2d_2+b_2c_2+\alpha\delta_2), \tag{44}$$

where the real parameters on the r.h.s. are defined by Eqs. (8). The imaginary value of the Lyapunov factor corresponds to a so-called *marginal* behavior, i.e., small perturbations oscillate with the constant amplitudes on the background of a fundamental soliton.

The imaginary Lyapunov factor $\delta\Omega_2$ given by Eq. (44) of the pump polariton 2 of the quasiphonon fundamental TWS's has the following physical origin. At the leading and trailing edges of the solitary LO phonon and polariton 1, i.e., at $|\tau|\gg\tau_s$ when $x_1\rightarrow 0$ and $z\rightarrow 0$, the coupling of these synchronous solitons with the polariton 2 is significantly reduced. Therefore, the pump wave should propagate as a free unperturbed polariton. On the other hand, the antidark (or gray) soliton in the cw profile of the pump polariton propagates with v_s, which for the quasiphonon TWS's strongly differs from the corresponding polariton group velocity v_{pol}. The large difference between v_s and v_{pol} results in the specific phase and amplitude modulations of the polariton 2 with the frequency $\delta\Omega_2$ of Eq. (44). Formally, these modulations do not destroy the fundamental solitons. However, numerical simulations show that small, but finite, perturbations can initiate a decay of the TWS's. Quasiphonon

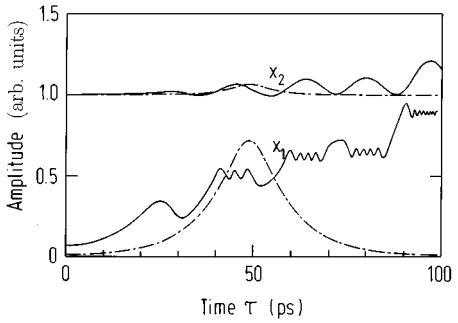

FIG. 10. The stability of the quasiphonon TWS's (the dispersion branch 3). The exact Raman resonance $\Delta\omega=0$, $\hbar\omega_{\mathbf{k}}=2.511$ eV $[\hbar(\omega_t-\omega_{\mathbf{k}}-\Omega_0)=3$ meV), and $\tau_s=10$ ps; $I_0=200$ MW/cm^2 — the stable TWS's (dash-dotted lines); $I_0=40$ MW/cm^2 — the unstable TWS's (solid lines). The initial perturbation at $\tau=0$ is $\delta x_2/x_{02}=0.025$.

TWS's, which are stable and unstable against a finite amplitude perturbation $\delta x_2/x_{02}=0.025$, are shown in Fig. 10. The amplitude modulation of the unstable pump polariton 2 of Fig. 10 (the upper solid line) indeed coincides with $\delta\Omega_2$ of Eq. (44).

Thus, the quasiphonon TWS's are stable only above a pump intensity threshold $I_{\rm th}^{(2)}(\omega,\omega_{\mathbf{k}},\tau_s)$. According to numerical simulations, for the given value of amplitude perturbation $(\delta x_2/x_{02}=0.025)$, one receives $I_{\rm th}^{(2)}\simeq 100-300$ MW/cm^2 and $I_{\rm th}^{(2)}\geqslant I_{\rm th}^{(1)}$. The frequency band of the stable quasiphonon solitons is located in the region of the anomalous dispersion of branch 3 and in the upper sectors of the spectral droplets 4–5 (see Fig. 2). These sectors of the quasiphonon branches 3–5 are the reminiscents of the unperturbed LO-phonon dispersion. The conditions (36a) and (36b) hold for $I_0>I_{\rm th}^{(1)}$ also, only for these frequencies. The soliton velocity v_s of the quasiphonon TWS's reaches a maximum value in this frequency band [see Fig. 7(b)].

The quasipolariton TWS's are stable within Eqs. (13a)–(13f) $(\mathrm{Re}\{\delta\Omega\}<0)$. Numerical simulations confirm this conclusion. However, for extremely high pump intensities $I_0\geqslant$ 0.5–1.0 GW/cm^2, the inequality Eq. (36c) does not hold and the quasipolariton TWS's should be analyzed with the generalized set of Eqs. (37a)–(37h). For these high intensities, the marginal behavior with the imaginary Lyapunov factor of Eq. (44) occurs also for quasipolariton TWS's.

The hypertransient regime of Eqs. (4a)–(4e) implies that the phonon-mediated nonlinearity is well developed in comparison with the corresponding damping constants Γ^x and $\Gamma^{\rm ph}$, i.e., the renormalized dispersion of the solitary polariton 1 is not masked by dephasing. The corresponding pump intensity threshold is the same as for the phonoriton effect and is about $I_0\simeq$ 10–50 MW/cm^2 for CdS.[11,15] Furthermore, in the hypertransient regime $\tau_s\leqslant\min\{(\Gamma^x/2)^{-1},(\Gamma^{\rm ph}/2)^{-1}\}=2/\Gamma^{\rm ph}$ for $T<77$ K. The typical coherence times $2/\Gamma^{\rm ph}$ of LO phonons are mainly due to the lattice anharmonicity and occur in the 10–30 ps scale.[28] This dictates the corresponding optimal values of the soliton duration τ_s.

The initial conditions appropriate for an effective generation of the polariton TWS's are beyond the scope of this paper. Our approach involves *two* external optical pulses in order to induce resonantly interacting polaritons. In a similar way as Raman solitons in para-H_2,[4–6] the polariton TWS's can probably be stimulated by introducing a π-phase seed in the long ''quasi-continuous-wave'' optical pulse, which transforms to the pump polariton. On the other hand, Raman solitons in molecular optics can also be formed from quantum noise of the *single* optical pump pulse in SRS.[8,5] Such a possibility is still unclear for the polariton TWS's.

For a pump intensity $I_0=100$ MW/cm^2 and $\omega_t-\omega_{\mathbf{k}}\simeq\Omega_0$, the concentration $N\propto x_{02}^2$ of virtual excitons in CdS is about 2×10^{17} cm^{-3}, according to Eq. (31). The corresponding Mott factor $Na_x^3\simeq0.6\times10^{-2}$ is still considerably less than unity, but exciton-exciton Coulombic interaction can already interfere with RRI. According to Keldysh's equations,[3] the additional cubic Kerr-type terms $\propto(|\widetilde{P}_1|^2+|\widetilde{P}_2|^2)\widetilde{P}_1$ and $\propto(|\widetilde{P}_1|^2+|\widetilde{P}_2|^2)\widetilde{P}_2$ will appear on the r.h.s. of Eqs. (10a) and (10c), respectively, due to Coulombic interaction. However, the polariton Raman TWS's are mainly determined by the quadratic *resonant* terms on the r.h.s. of Eqs. (10a)–(10c). This conclusion resembles the argument in theory of superconductivity, that the Coulomb electron-electron nonresonant interaction does not destroy phonon-mediated coherent pairing.

The Raman TWS's can be generated not only in polar semiconductors with strong exciton–LO-phonon Fröhlich interaction. Conjugated polymers are also well suited for the Raman TWS's, due to their extremly large phonon-mediated optical nonlinearities.[25] For example, quasi-one-dimensional polydiacetylene – para-toluene-sulfonate (PDA-pTS), which is a quasi-one-dimensional semiconductor, can be prepared in a high-quality single crystalline form.[26] The lowest exciton state of this polymer exhausts most of the interband oscillator strength and is well separated in energy from any other dipole-active electronic excitation. The phonon-mediated optical Stark effect (phonoriton renormalization) has been already observed in PDA-pTS.[12] Within our model, the main specific feature of PDA-pTS is nonpolar exciton-phonon interaction. Although in this case the matrix element $M_{x\text{-ph}}$ is independent of the phonon wave number $\mathbf{p}-\mathbf{k}$, the dispersion equation for the nonlinear polariton 1 has the same order and form as Eq. (29a). Therefore, the developed classification of the TWS's by the dispersion of the solitary polariton 1 is still correct. The quasiphonon dispersion branch *3* stems from the unique evolution of the initial unperturbed dispersions towards the modified spectrum (see Fig. 2), i.e., is an universal property of Eq. (29a).

Raman spectroscopy of the exciton states has been developed in detail for III-V compound semiconductors.[18,27] For these semiconductors, e.g., GaAs, the assumption of the single intermediate exciton resonance $(n=1)$ is broken,[19] at least for the pump polariton 2, due to $\Omega_0>\Omega_c>\epsilon^x$. This means that bound and ionized (continuum) exciton states[29] have to be included in the initial Hamiltonian (1) and in the polarization Eq. (4e). Moreover, allowed and forbidden scattering can interfere.[18] Both of these corrections complicate the modeling of Raman TWS's.

VIII. CONCLUSIONS

In this paper, we develop the theory of coupled three-wave solitons in resonant Raman interaction of two coherent

intense polaritons, due to the Fröhlich mechanism. The following conclusions summarize our analysis.

(i) A closed set of the five nonlinear macroscopic equations for the photon and exciton components of two polaritons and for the corresponding resonant LO phonon is derived self-consistently on the basis of the exciton-photon – LO-phonon microscopic Hamiltonian. A mathematical approach, which treats within the initial microscopic model the polariton effects, as well as the entire series of $\chi^{(n)}$, is developed for the fundamental Raman TWS's.

(ii) The classification of fundamental polariton TWS's is given in accordance with the dispersion of the solitary polariton of the resonant triplet. Quasipolariton and quasiphonon Raman solitons are formed. The quasiphonon TWS's have no analogy in classical nonlinear optics.

(iii) The quasipolariton TWS's are attributed to the polaritonlike dispersion branches of a solitary polariton. For these coupled nonlinear waves, a gray soliton in the cw background of the pump polariton is formed in forward scattering RRI, while in the backscattering geometry an antidark soliton is found. A solitary polariton of the quasipolariton TWS's is a giant parametric pulse of the nonlinear resonant triplet.

(iv) The quasiphonon TWS's refer to those dispersion branches that are the ''topological reminiscents'' of the unperturbed LO-phonon dispersion $\omega_{\mathbf{k}}+\Omega_0$. These quasiphonon Raman TWS's propagate with an anomalously small velocity ($v_s \simeq 10^5$ cm/s), are accompanied by a giant solitary LO phonon, and are stable only in a close vicinity of the Raman resonance for the pump intensities $I_0 \geqslant 100$–300 MW/cm^2.

ACKNOWLEDGMENTS

We appreciate valuable discussions with L.V. Keldysh. This work was supported by the Volkswagen Stiftung and by the NATO Collaborative Research Grant No. 930084.

[1] J. Goll and H. Haken, Phys. Rev. A **18**, 2241 (1978); S.N. Belkin, P.I. Khadzhi, S.A. Moskalenko, and A.H. Rotaru, J. Phys. C **14**, 4109 (1981); K. Watanabe, H. Nakano, A. Honold, and Y. Yamamoto, Phys. Rev. Lett. **62**, 2257 (1989); K.T. Stoychev and M.T. Primatarowa, Phys. Rev. B **46**, 10 727 (1992); I.B. Talanina, M.A. Collins, and V.M. Agranovich, Solid. State Commun. **88**, 541 (1993); Phys. Rev. B **49**, 1517 (1994).

[2] S. Schmitt-Rink, D.S. Chemla, and H. Haug, Phys. Rev. B **37**, 941 (1988).

[3] L.V. Keldysh, in *Problems in Theoretical Physics*, edited by V.I. Ritus (Nauka, Moscow, 1972), p. 433.

[4] K. Druhl, R.G. Wentzel, and J.L. Carlsten, Phys. Rev. Lett. **51**, 1171 (1983); K. Druhl, J.L. Carlsten, and R.G. Wentzel, J. Stat. Phys. **39**, 615 (1985); R.G. Wentzel, J.L. Carlsten, and K. Druhl, *ibid.* **39**, 621 (1985).

[5] D.C. MacPherson, J.L. Carlsten, and K. Druhl, J. Opt. Soc. Am. B **4**, 1853 (1987); D.C. MacPherson, R.C. Swanson, and J.L. Carlsten, Phys. Rev. A **39**, 6078 (1989); **40**, 6745 (1989).

[6] K. Midorikawa, T. Tashiro, Y. Akiyama, and M. Obara, Phys. Rev. A **41**, 562 (1990); Y. Akiyama, K. Midorikawa, M. Obara, and T. Tashiro, J. Opt. Soc. Am. B **8**, 2459 (1991).

[7] F.Y.F. Chu and A.C. Scott, Phys. Rev. A **12**, 2060 (1975); D.J. Kaup, Physica D **6**, 143 (1983); **19**, 125 (1986); H. Steudel, *ibid.* **6**, 155 (1983); Opt. Commun. **57**, 285 (1986); C.R. Menyuk, Phys. Rev. Lett. **62**, 2937 (1989).

[8] J.C. Englund and C.M. Bowden, Phys. Rev. Lett. **57**, 2661 (1986); C.M. Bowden and J.C. Englund, Opt. Commun. **67**, 71 (1988).

[9] J.J. Hopfield, Phys. Rev. **112**, 1555 (1958); J.J. Hopfield and D.G. Thomas, *ibid.* **132**, 563 (1963).

[10] J.A. Armstrong, N. Bloembergen, J. Ducuing, and P.S. Pershan, Phys. Rev. **127**, 1918 (1962); S.A. Akhmanov, A.S. Chirkin, K.N. Drabovich, A.I. Kovrigin, R.V. Khokhlov, and A.P. Sukhorukov, IEEE J. Quantum Electron. **QE-4**, 598 (1968); J.A. Armstrong, S.S. Jha, and N.S. Shiren, **QE-6**, 123 (1970).

[11] A.L. Ivanov and L.V. Keldysh, Zh. Eksp. Teor. Phys. **84**, 404 (1983) [Sov. Phys. JETP **57**, 234 (1983)]; A.L. Ivanov, *ibid.* **90**, 158 (1986) [**63**, 90 (1986)]; G.S. Vygovskii, G.P. Golubev, E.A. Zhukov, A.A. Fomichev, and M.A. Yakshin, Pis'ma Zh. Eksp. Teor. Phys. **42**, 134 (1985) [JETP Lett. **42**, 164 (1985)].

[12] B.I. Greene, J.F. Mueller, J. Orenstein, D.H. Rapkine, S. Schmitt-Rink, and M. Thakur, Phys. Rev. Lett. **61**, 325 (1988); in *Proceedings of the NATO Workshop on Optical Switching in Low-Dimensional Systems, Marbella, Spain, 1988*, Vol. 194 of *NATO Advancd Study Institute, Series B: Physics*, edited by H. Haug and L. Banyai (Plenum Press, New York, 1989), p. 97.

[13] T. Ishihara, J. Phys. Soc. Jpn. **57**, 2573 (1988).

[14] J.L. Birman, M. Artoni, and B.S. Wang, Phys. Rep. **194**, 367 (1990); B.S. Wang and J.L. Birman, Solid State Commun. **75**, 867 (1990); Phys. Rev. B **42**, 9609 (1990).

[15] A.L. Ivanov, Solid State Commun. **74**, 383 (1990); D.Sc. thesis, Moscow State University, Moscow, 1991.

[16] N.M. Khue, N.Q. Huong, and N.H. Quang, J. Phys Condens. Matter **6**, 3221 (1994).

[17] K. Emu and M. Kuwata-Gonokami, Phys. Rev. Lett. **75**, 224 (1995).

[18] M. Cardona, in *Light Scattering in Solids VI*, edited by M. Cardona and G. Güntherodt, Topics in Applied Physics Vol. 50 (Springer, Berlin, 1982), p. 19.

[19] C. Trallero-Giner, A. Cantarero, and M. Cardona, Phys. Rev. B **40**, 4030 (1989).

[20] A.I. Ansel'm and Yu.A. Firsov, Zh. Eksp. Teor. Phys. **30**, 719 (1956) [Sov. Phys. JETP **3**, 564 (1957)]; Y. Toyozawa, Prog. Theor. Phys. **20**, 53 (1958).

[21] R.M. Martin and T.C. Damen, Phys. Rev. Lett. **26**, 86 (1971); R.M. Martin, Phys. Rev. B **4**, 3676 (1971); S.A. Permogorov and A.N. Reznitsky, Solid State Commun. **18**, 781 (1976).

[22] A.K. Ganguly and J.L. Birman, Phys. Rev. **162**, 806 (1967); R. Zeyher, C.S. Ting, and J.L. Birman, Phys. Rev. B **10**, 1725 (1974).

[23] Yu.S. Kivshar, IEEE J. Quantum Electron. **EQ-29**, 250 (1993).

[24] D.J. Kaup, A. Reiman, and A. Bers, Rev. Mod. Phys. **51**, 275 (1979).

[25] *Nonlinear Optical Properties of Organic Molecules and Crystals*, edited by D.S. Chemla and J. Zyss (Academic Press, Orlando, 1987), Vol. 2.

[26] D.N. Batchelder and D. Bloor, J. Phys. C **15**, 3005 (1982).

[27] J. Menendez and M. Cardona, Phys. Rev. Lett. **51**, 1297 (1983); W. Kauschke and M. Cardona, Phys. Rev. B **33**, 5473 (1986); W. Kauschke, V. Vorlicek, and M. Cardona, *ibid.* **36**, 9129 (1987).

[28] L.K. Vodop'yanov and E.A. Vinogradov, Fiz. Tverd. Tela **16**, 1432 (1974) [Sov. Phys. Solid State **16**, 919 (1973)]; D. von der Linde, J. Kuhl, and H. Klingenberg, Phys. Rev. Lett. **44**, 1505 (1980); J. Menendez and M. Cardona, Phys. Rev. B **29**, 2051 (1984); J.A. Kash and J.C. Tsang, in *Light Scattering in Solids VI*, edited by M. Cardona and G. Güntherodt, Topics in Applied Physics Vol. 68 (Springer, Berlin, 1991), p. 423.

[29] H. Haug and S.W. Koch, *Quantum Theory of the Optical and Electronic Properties of Semiconductors* (World Scientific, Singapore, 1990), Sec. 10.